SYMMETRICAL VOLTAGE DIP ANALYSIS FOR DOUBLY FED INDUCTION GENERATOR

A thesis is submitted to fulfil the requirement of the degree
Master in Electrical Engineering

Submitted by
SUSNATA KANJILAL

Examination Roll no. – M4ELE24004

Registration no. – 163479 of 2022-2023

Year – 2nd, Semester – 4th
Under the Guidance of
Prof (Dr.) Debashis Chatterjee
Prof Nikhil Mondal
Prof Mihir Hembram

Department of Electrical Engineering Jadavpur University
Kolkata – 700032
August 2024

Faculty of Engineering and Technology Jadavpur University, Kolkata - 700032

Certificate

This is to certify that the thesis entitled “Analysis of Stator Active and Reactive Power in a Doubly fed Induction Generator” submitted by Susnata Kanjilal (Examination Roll No: M4ELE23002), under our supervision and guidance during the session of 2022-24 in the department of Electrical Engineering, Jadavpur University. We are satisfied with his work, which is being presented for the partial fulfilment of the degree of Master in Electrical Engineering from Jadavpur University, Kolkata-700032.

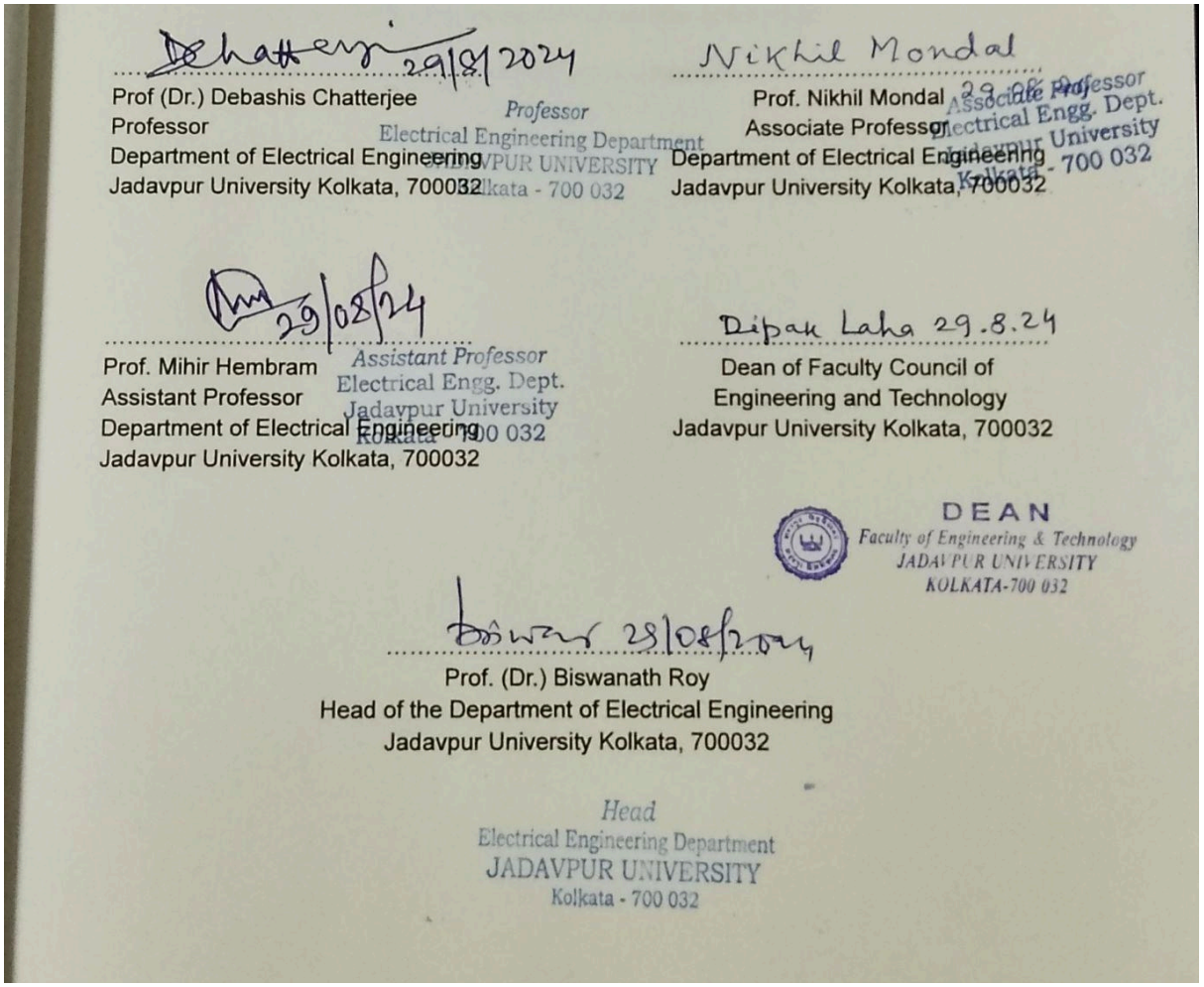

Faculty of Engineering and Technology Jadavpur University, Kolkata - 700032

Certificate of Approval

The forgoing thesis entitled “Symmetrical voltage dip analysis for Doubly fed Induction Generator” is hereby approved as a creditable study of an Engineering subject carried out and presented in a manner that fulfils its acceptance as a prerequisite to the degree for which it is submitted. It is understood that by this approval, the undersigned does not necessarily endorse or approve any statement made, opinion expressed, or conclusion drawn therein but approves the thesis only for the purpose for which it is submitted.
The final examination for evaluation of the thesis

Signature of the examiners
……
……
……
…….

Declaration of Originality

I hereby declare that this thesis contains original research work done by me. All the information in this document has been obtained and presented according to academic rules and ethical conduct. I also declare that, as required by these rules and conduct, I have fully cited and referenced all material and results that are not original to this work.

Name: SUSNATA KANJILAL
Examination Roll No: M4ELE24004
University Registration No: 163479 of 2022-23
Thesis Title: Symmetrical voltage dip analysis for Doubly fed Induction Generator

Signature with Date

ACKNOWLEDGEMENTS

I express my sincere gratitude to my supervisor, Prof.Dr. Debashis Chatterjee for his encouragement, suggestion, and advice, without which it would not have been possible to complete my thesis successfully. I would like to thank Prof. Nikhil Mondal and Prof Mihir Hembram for being a constant source of encouragement, inspiration and for their valuable suggestions coupled with their technical expertise throughout my research work. It was a great honour for me to pursue my research under their supervision.

I would also like to thank my coworker Sanju Sardar, all the staff of the Drives and Simulation laboratory, and the research scholars of our department, specially Subinoy, for providing constant encouragement throughout my thesis work.

Finally, I extend my words of gratitude to my parents for personally motivating me to carry out the work smoothly.

ABSTRACT

This thesis carries out a theoretical analysis and simulation of the dynamic behaviour of the doubly-fed induction machine during grid disturbances and also analyses the various strategies taken up to mitigate the adverse effects.During normal operation, the rotor's induced emf is small and proportional to the slip. However, under a voltage dip, the induced emf becomes significantly larger, influenced by rotational speed and voltage transients. In a total three-phase voltage dip, although the stator voltage drops to zero, the machine remains temporarily magnetised, creating what is known as natural flux, which is not generated by any stator voltage.The natural flux is fixed with the stator and from the rotor frame of reference is seen as a flux that rotates inversely at the rotor speed.As a consequence, the natural flux induces an emf much greater than those appearing during regular operation. This voltage is not proportional to the slip, but to the rotor speed.

CONTENTS

CHAPTER 1

INTRODUCTION

1.1 MOTIVATION FOR WORK:

The world is currently facing an energy crisis. Since the beginning of industrialization, energy demand has increased exponentially, leading to the overuse of non-renewable resources like coal and petroleum. This overconsumption has not only depleted non-renewable energy sources but also caused severe pollution. To address these issues, nations worldwide, including India, have prioritised the development and utilisation of green renewable energy. The rising demand for electricity, global warming, and excessive carbon emissions have driven the growth of green and cost-effective energy generation sources globally, including the development of wind energy. The development of the wind energy green era has also resulted from this.

In recent years, India has significantly increased its adoption of green energy, as providing conventional energy to a population nearing 1.4 billion becomes increasingly challenging. Graphical data shows the rise in green energy usage in India, with Gujarat reaching nearly 18,000 MW of renewable energy by 2022, equally divided between solar and wind sources. Hence it can be inferred that the use of wind as a dominant form of energy is slowly making giant strides in India.

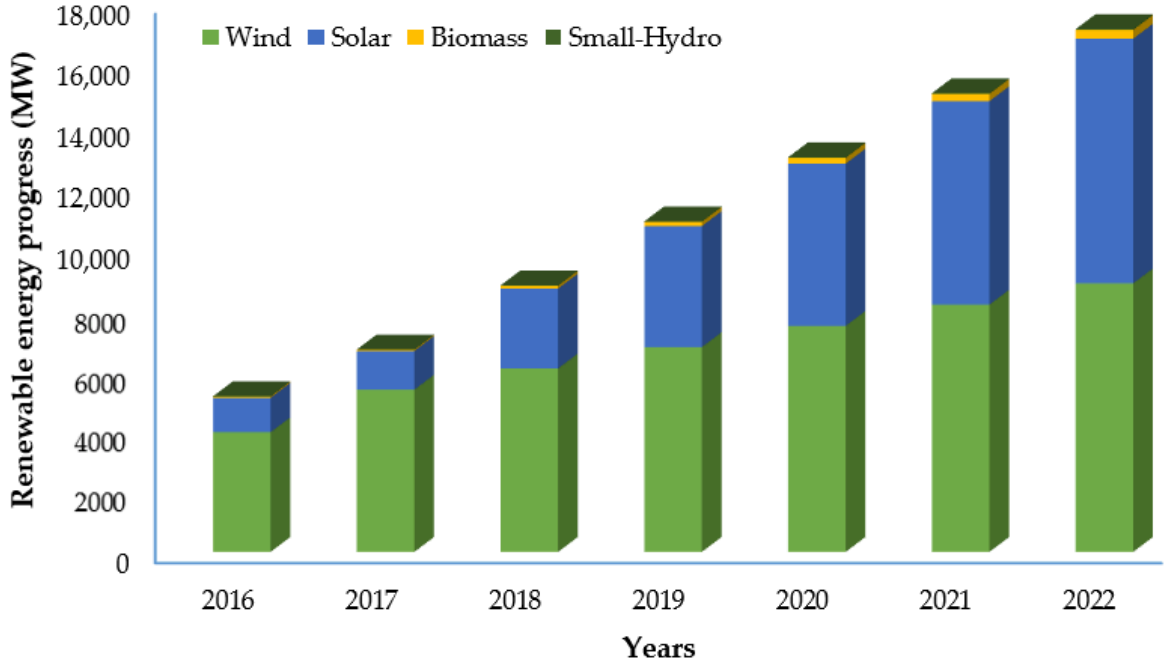

Fig: 1.1 (a): Increasing use of green energy in Gujrat

In the Union Budget, 2023, one of the main Saptarishis (7 targets for 2023) was enhancement of renewable energy in India.As of Feb 2023, Renewable energy sources, including large hydropower, have a combined installed capacity of 178.79 GW.
The following is the installed capacity for Renewables:

- Wind power: 42.6 GW
- Solar Power: 66.7 GW
- Biomass/Cogeneration: 10.2 GW
- Small Hydro Power: 4.94 GW
- Waste To Energy: 0.55 GW
- Large Hydro: 46.85 GW

India aims to produce five million tonnes of green hydrogen by 2030, supported by 125 GW of renewable energy capacity. The rapid growth of the wind energy sector in India provides strong motivation to study various aspects of wind energy generation.

Wind energy is derived from the flow of wind. Harnessing this energy is relatively inexpensive, and as a green, renewable source, it exerts less environmental pressure. This form of energy is efficient and reduces the reliance on fossil fuels, leading to the development of associated wind energy generation technologies, such as wind turbines. Wind turbines are categorised into two main types: Fixed Speed Wind Turbines (FSWT) and Variable Speed Wind Turbines (VSWT).

As wind power penetration increases, it becomes crucial to ensure that wind power generation does not negatively impact power quality, security, and reliability in power systems, both during steady-state operation and under contingency scenarios. Dynamic performance requirements for grid-connected wind turbines focus on the turbine's ability to remain operational during a voltage dip, known as fault ride-through (FRT). FRT requirements may include provisions for reactive power support to assist with voltage stability.

In contemporary applications, particularly in the renewable energy sector, DFIGs are valued for their ability to operate at variable speeds, a crucial feature for wind turbines. Unlike traditional wind turbines that operated at a fixed speed, modern wind turbines must adjust to varying wind speeds to maximise efficiency. This necessity has driven the adoption of DFIGs in wind turbines, allowing for operation at speeds above or below synchronous speed, thus accommodating variable slip speeds.

1.2 LITERATURE REVIEW:

The origins of Doubly Fed Induction Generators (DFIG) can be traced back to wound rotor induction motors with multiphase winding sets on both the rotor and stator, invented by Nikola Tesla in 1888. Initially, the rotor winding set of the doubly fed electric machine was connected to variable resistors via multiphase slip rings for starting purposes, leading to the loss of slip power in the resistors. To enhance efficiency during variable speed operations, methods were developed to recover this

slip power. Krämer drives, for example, connected the rotor to an AC and DC machine set that then fed a DC machine linked to the slip ring machine's shaft.However in Kramer drives the power-flow is unidirectional and can be operated only in the sub-synchronous speed region.

The Doubly Fed Induction Generator (DFIG) utilising an AC-AC converter in the rotor circuit, also known as the Scherbius Drive, has long been a preferred choice for high-power applications with a limited speed range. In this configuration, the power converter is designed to handle only the rotor power, which is approximately one-third of the stator power. The vector-control scheme used to manage the AC-AC converters enables independent control of torque and rotor excitation current, along with decoupled control of the active and reactive power drawn from the grid supply[4].

The Scherbius DFIG system is naturally suited for wind generation due to its restricted speed range (from cut-off to rated wind velocity). Most reported Scherbius DFIG systems employ either a current-fed DC-Link converter or a cycloconverter in the rotor circuit. However, the current-fed DC-Link converter has several drawbacks: the DC-Link choke is costly, an extra commutation circuit is needed for operation at synchronous speed (which is the operational speed range), leading to poor performance at low slip speeds, and it draws rectangular current waveforms from the supply, introducing unwanted harmonics.
A vector-controlled Scherbius scheme with a 6/3-pulse cycloconverter can address the synchronous speed problem. However, this cycloconverter scheme also have the disadvantage of requiring a transformer for voltage matching in addition to a naturally commutated DC-Link. These disadvantages can be overcome by using two PWM/SVPWM voltage-fed current-regulated inverters connected back-to-back in the rotor circuit. The typical characteristics of such a Scherbius scheme, with both converters controlled, include:

- Operation below, above, and through synchronous speed, with the speed range restricted only by the rotor-voltage ratings of the DFIG.
- Operation at synchronous speed, with DC currents injected into the rotor and the inverter working in chopping mode.
- Low distortion in stator, rotor, and supply currents.
- Independent control of generator torque and rotor excitation.
- Control of the displacement factor between voltage and current in the supply converter, and hence control over the system power factor.

Thus, a DFIG with PWM/SVPWM voltage-fed current-regulated inverters connected back-to-back in the rotor circuit provides characteristics similar to a conventional generator, making it suitable for effective connection to the main grid. Today, frequency changers used in applications up to several tens of megawatts consist of two back-to-back connected IGBT inverters[4].

Additionally, several brushless concepts have been developed to eliminate the need for slip rings, which require maintenance. The DFIG with a back-to-back converter is a system frequently used in wind turbines. Traditional wind turbines operate at fixed speeds, while DFIG allows for variable speed operation. The back-to-back converter, connected to the rotor of the DFIG, feeds the rotor with currents of varying frequency to achieve the desired rotor speeds. This document demonstrates the implementation of a DFIG wind turbine with a back-to-back converter controller. The simulation cases cover the response of stator active and reactive power in a DFIG at two different rotor speeds: one at sub-synchronous speed and the other at super-synchronous speed.One of the main advantages of the DFIM is that it provides variable speed using a small and economic power converter.However, as wind energy penetration increased and the number of wind turbines using the DFIM expanded, the main DFIM disadvantage became more and more relevant: its excessive sensitivity to electric grid disturbances.A Drop of one or more phase voltages can be especially damaging for the electronic converter. A voltage dip causes overcurrents and overvoltages in the rotor windings, which would damage the converter connected to their terminals if no countermeasures were taken.voltage dips and generally any perturbation of the grid voltage cause the induced rotor electromagnetic force (emf) to increase notably. Such overvoltage negatively affects the machine regulation loops and in the case of severe voltage dips, it may cause the rotor converter to saturate and hence lose control of the machine[1].

In summary,based on the literature, the first issue that has been addressed in the dissertation is the development of the matlab simulation file of a DFIG based WECS using Field oriented control. Later a voltage dip is created at the grid terminal and the dynamical behaviour of the DFIG is recorded. And finally these behaviours are compared with that of a system having an active crowbar protection.

1.3 ORGANISATION OF THESIS

The entire thesis is completed in seven (7) chapters.

o Chapter 1: outlines the preliminary concept of thesis work. It contains a brief history of Doubly fed induction Generator, my motivation for this work and an outlook about the different chapters and topic of discussion in this thesis.

o Chapter 2: Chapter 2 deals with the analysis of a wind turbine, a block diagram including the mechanical and electrical sections and discussion of each block. It also deals with the different types of wind turbines, with special emphasis on the working and structure of type 3 DFIG based wind turbines.

o Chapter 3: Chapter 3 deals with the working of DFIG, the various operating curves and principles associated with it. It also discusses the equivalent mathematical circuit, and the nature of power flow.

o Chapter 4: This chapter mainly outlines the back to back converter used in DFIG. This chapter also discusses the super-synchronous and sub-synchronous nature of motoring and generating action.

o Chapter 5: Chapter 5 deals with analysis of symmetrical voltage dips occurring at the grid terminals of the DFIG based VSWT. It also outlines the remedy for such issues.

o Chapter 6:This chapter deals with the entire matlab modelling of DFIG based VSWT with FOC. Here the modelling of the stator side, rotor side of the DFIG is discussed, as well as outlining the modelling of crowbar protection etc.

o Chapter 7: This chapter contains the graphical results of various cases. The graphs contain initial transient state and final steady state. This chapter also outlines some conclusions and different avenues for future work.

CHAPTER 2

ANALYSIS OF WIND TURBINE

2.1 INTRODUCTION:

A wind turbine transforms kinetic energy from the wind into mechanical energy. This mechanical energy is then converted into electrical energy by generator units. The electrical energy is transferred into the utility grid using a power electronic converter and step-up transformers, and finally delivered to the end users. A fundamental concept in understanding wind technology is wind energy capture. Wind holds in it a discrete amount of power at any given point in time, dependent in large part on the wind speed.

Wind energy is captured by the turbine's rotor blades, which are designed to have an aerodynamic shape to maximise energy capture.The kinetic energy of the wind causes the rotor blades to spin around a central hub. The spinning motion converts the wind's kinetic energy into mechanical energy in the form of rotational motion.

The rotational motion of the rotor is transferred to the main shaft, which is connected to the rotor hub.The main shaft is connected to a gearbox (in some designs) that increases the rotational speed of the shaft to match the optimal speed of the generator.

As wind speed can vary greatly, wind turbines must be capable of operating over a wide wind speed range. The wind turbine can operate in one of two ways. The first is to have a relatively fixed rotational speed, in which an increase in wind speed can slightly increase the rotor speed above the synchronous speed and thus varying the slip. This is based purely on the torque-speed relationship of an induction machine. The wind turbine can also operate as a variable-speed machine, varying the rotor speed based on the wind velocity. A speed controller is used to vary the pitch of the wind turbine blades during high wind speeds to reduce the power intake and protect the wind turbine, In which case the rotor speed is also controlled in order to optimise the ratio of wind speed to rotor speed. The goal in varying the pitch is to maximise efficiency by optimising a term called the tip-speed ratio. The tip-speed ratio () is defined as:

$$\boldsymbol{\lambda} = \frac{V_{tip}}{V_{wind}} \tag{2.1}$$

where v_{tip} is the velocity of the blade tip and v_{wind} is the wind velocity. The tip speed velocity can be calculated from:

$$\mathbf{v_{tip}} = \Omega \times r \tag{2.2}$$

where , Ω is the mechanical speed of the wind turbine and r is the radius of the circle of rotation, in this case the length of the wind turbine blade. From here it can be seen

that the ability to maximise the aerodynamic efficiency of energy capture, is directly related to the ability to vary the rotational speed. There are several configurations for variable speed wind turbines that allow for the generator's rotor to operate at a variable rotational speed. The various configurations for fixed and variable speed wind turbine generators can be broken down into four main types to be described in the following sections:

1. Fixed Speed Wind Turbine (FSWT) with induction generator
2. Variable Speed Wind Turbine (VSWT) with variable rotor resistance
3. VSWT with Doubly-Fed Induction Generator (DFIG)
4. VSWT with Full-Power Converter (FPC)

There are common components with each of the configurations as seen in the figures for each. A gear box is used in between the wind turbine and generator to convert the lower rotational speed of the turbine to a higher rotational speed for the generator rotor. Also, a step-up transformer is used to connect the wind turbine generator to the grid, transforming the voltage up as needed to connect to the distribution or transmission system.

2.1.1 Fixed Speed Wind Turbine:

The generator rotor rotates at a fixed speed based on the grid frequency and pole pairs, causing the turbine rotor to also rotate at a fixed speed. Capacitor banks provide local reactive power to reduce grid demand. Wind power variations lead to fluctuating power delivery, affecting grid power quality.

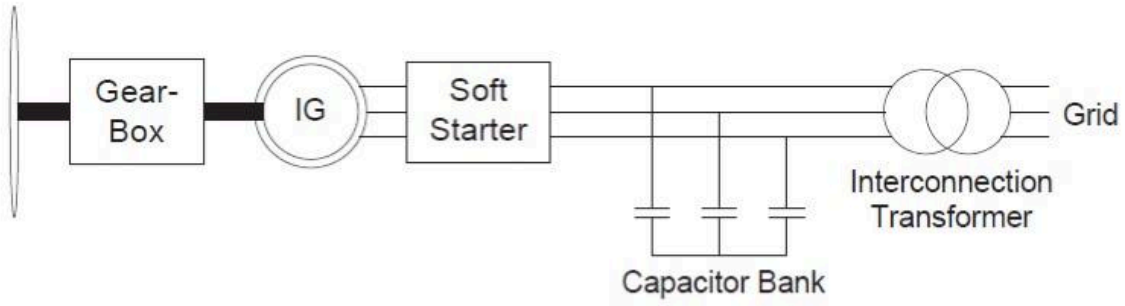

FIGURE 2.1: *Type 1 DFIG based VSWT*

Figure shows a fixed-speed wind turbine connected to the grid via an induction generator, with stator terminals directly linked to the grid.

2.1.2 Variable Speed Wind Turbine with Variable Rotor Resistance:

In this configuration, the rotor resistance can be adjusted by connecting resistors to the rotor terminals via slip rings, allowing control over the rotor speed and creating a variable speed wind turbine (VSWT). Capacitor banks are still necessary to compensate for reactive power consumption. However, this setup only allows for rotor speeds above synchronous speed and results in wasted energy as excess energy is diverted through the resistors.

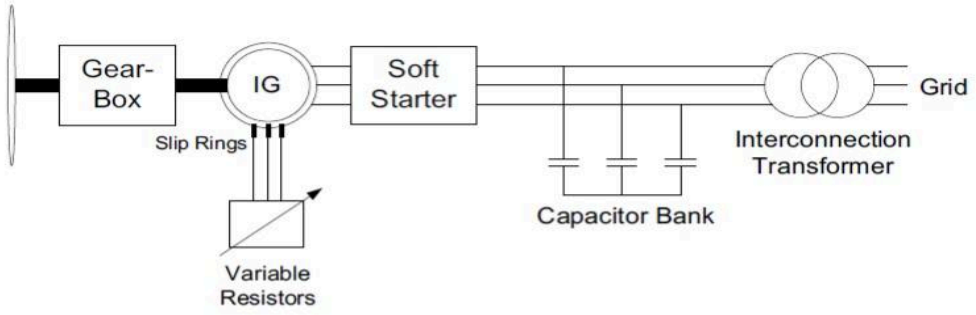

FIGURE 2.2: Type 2 DFIG based VSWT

2.1.3 Variable Speed Wind Turbine with Doubly Fed Induction Generator:

In this setup, the stator terminals are directly connected to the grid, and the rotor windings are connected to a three-phase voltage source converter via slip rings. This means both the stator and rotor are linked to the grid, hence the term "doubly-fed" generator. Like previous configurations, a step-up transformer is used to elevate the stator and rotor voltages to match the grid voltage. Here, a three-winding transformer is employed to couple both the stator and rotor with the grid.

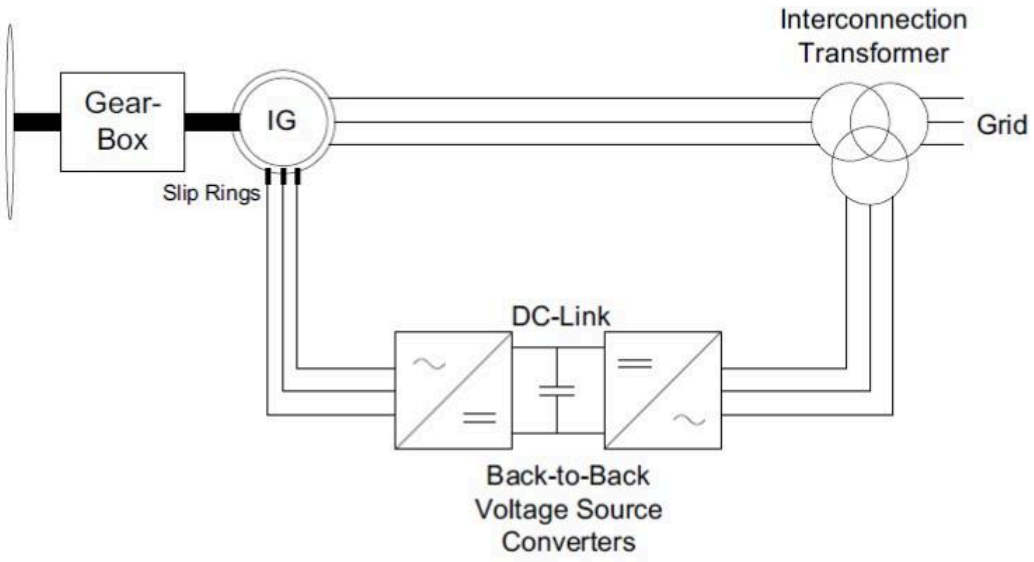

FIGURE 2.3: Type 3 DFIG BASED VSWT

2.1.4 Variable Speed Wind Turbine with Full Power Converter (FPC):

Back-to-back Voltage Source Converters (VSCs) are connected directly to the generator's stator terminals, whether it's an induction or synchronous generator. All

power flows through these converters to the grid, requiring them to be rated for the generator's full capacity, necessitating larger components. The setup connects to the grid via a step-up transformer, and an AC filter is typically included before the point of common coupling,

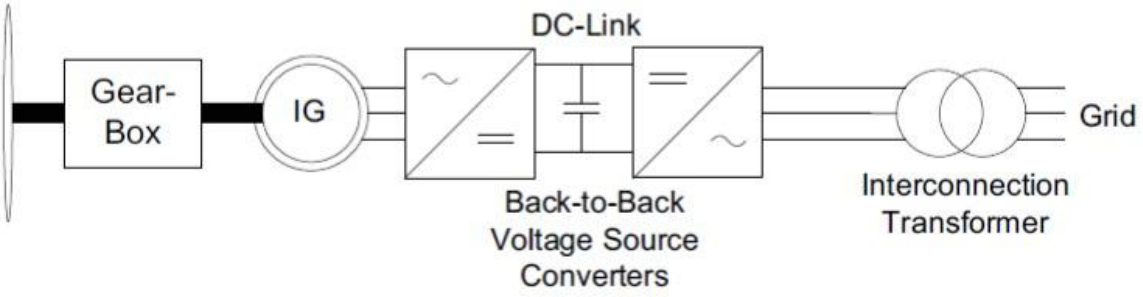

FIGURE 2.4: Type 4 DFIG based VSWT

Figure shows a Variable Speed Wind Turbine (VSWT) with a full power converter. With the FPC, the machine-side converter can be used to give full controllability of the rotor speed, making this system very flexible.

2.2 FIXED SPEED WIND TURBINE (FSWT):

The basic components of a wind turbine are described by means of a fixed speed wind turbine, based on a squirrel cage (asynchronous machine) and stall–pitch power control.Fixed Speed Wind Turbines (FSWT) operate at a quasi-fixed mechanical speed, largely independent of wind speed, due to their connection to a fixed frequency electrical network. This technology, primarily developed in Denmark during the late 1970s, became widespread in the 1980s and 1990s. Notable manufacturers include Vestas, Bonus (Siemens), Nordex, and Repower.
Components and Operation:

- **Nacelle:** Houses key components like the gearbox and electrical generator. Service personnel access the nacelle from the tower.
- **Rotor Blades:** Capture wind and transfer its power to the rotor hub. Designed like aeroplane wings, they include movable blade tips (tip brakes) that act as air brakes.
- **Stall and Pitch Control:** Methods to limit or control the power extracted from the wind, where stall control is based on blade design and pitch control involves adjusting the angle of the blades.

The aerodynamics of Fixed Speed Wind Turbines (FSWT) are crucial for their operation and efficiency. The main components of an FSWT, such as the rotor blades, hub, gearbox, and generator, are designed to capture and convert wind energy into mechanical and electrical energy effectively.The aerodynamic design of

FSWTs is aimed at ensuring efficient energy capture while maintaining structural integrity and safety under varying wind conditions. The choice between passive and active stall control, as well as the use of pitch control, reflects different engineering approaches to optimising wind turbine performance.

- The rotor blades act like a porous disk that captures the wind and reduces its momentum. This process involves a pressure difference across the disk and a deflection of downstream airflows. The blades are aerodynamically shaped and twisted along their longitudinal axis to ensure gradual stalling rather than abrupt stalling at critical wind speeds.
- The power available in the wind is expressed as kinetic energy passing through an area (A1) at a speed (Vv). The formula for this power (Pv) is:

$$Pv = \frac{1}{2}\rho A_1 V_v^3 \text{ , where } \rho \text{ is the air density.} \quad (2.3)$$

- The wind turbine can only extract a portion of this power, represented by:

$$P_t = \frac{1}{2}\rho\pi R^2 V_v^3 C_p \quad (2.4)$$

where R is the radius of the turbine and Cp is the power coefficient, a dimensionless parameter indicating the efficiency of the wind turbine in converting wind energy into mechanical energy.The theoretical maximum value of Cp is given by the Betz limit, which is approximately 59.3%

- The power coefficient depends on wind speed, the rotor's rotational speed, and the pitch angle of the blades. It is often expressed as a function of the tip speed ratio (λ)

$$\lambda = \frac{R\Omega_t}{V_v} \quad (2.5)$$

Where Ω_t is the angular speed of the rotor.

- The torque generated by the rotor (Tt) is obtained from the power received and the rotational speed of the turbine:

$$T_t = \frac{P_t}{\Omega_t} = \frac{\rho\pi R^2 V_v^3}{2\Omega_t} C_p = \frac{\rho\pi R^3 V_v^2}{2\lambda} C_p = \frac{\rho\pi R^3 V_v^2}{2} C_t \quad (2.6)$$

Where, C_t is the torque coefficient**.**

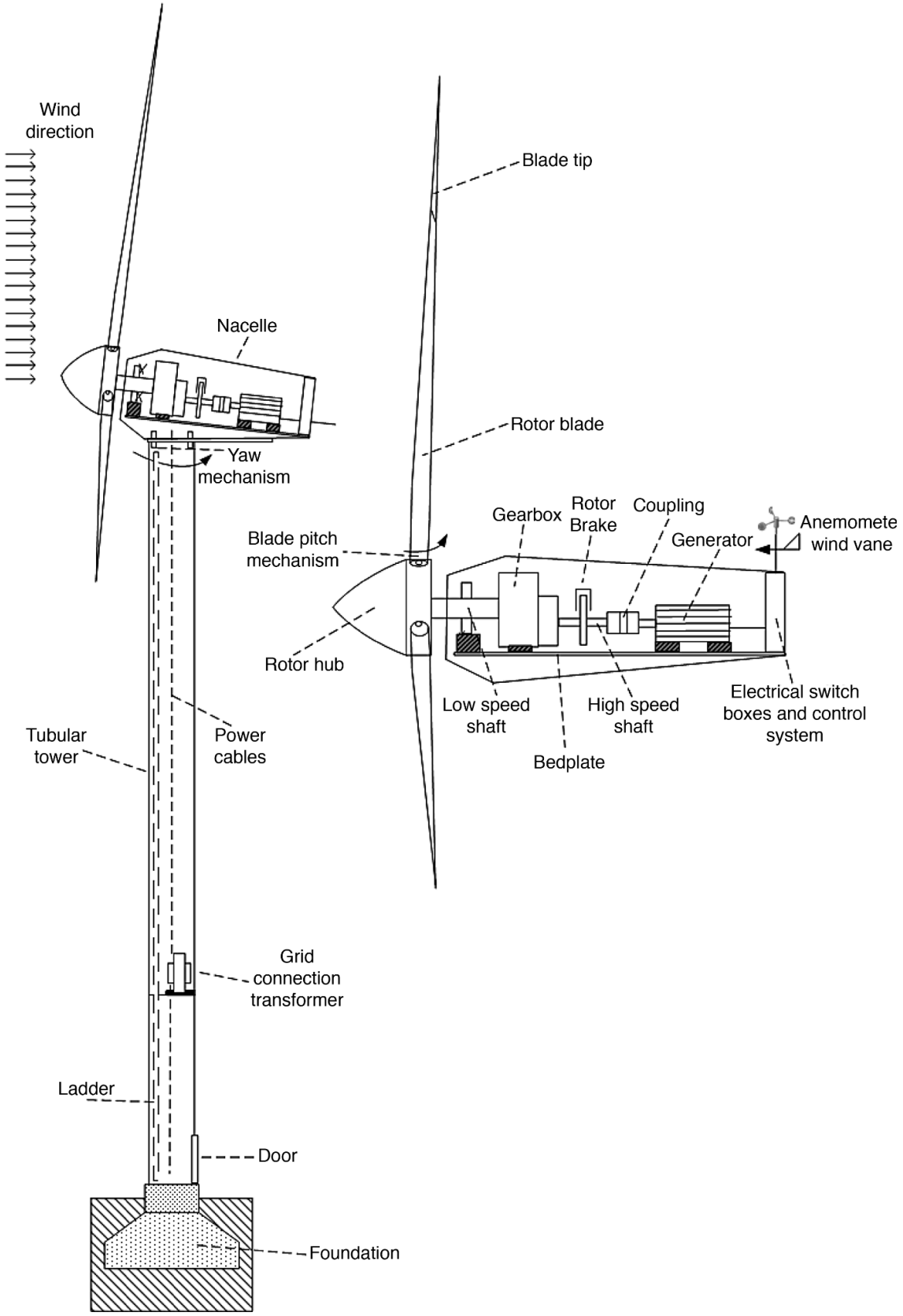

FIGURE 2.5 : Main components of a fixed speed wind turbine.

2.3 VARIABLE SPEED WIND TURBINE:

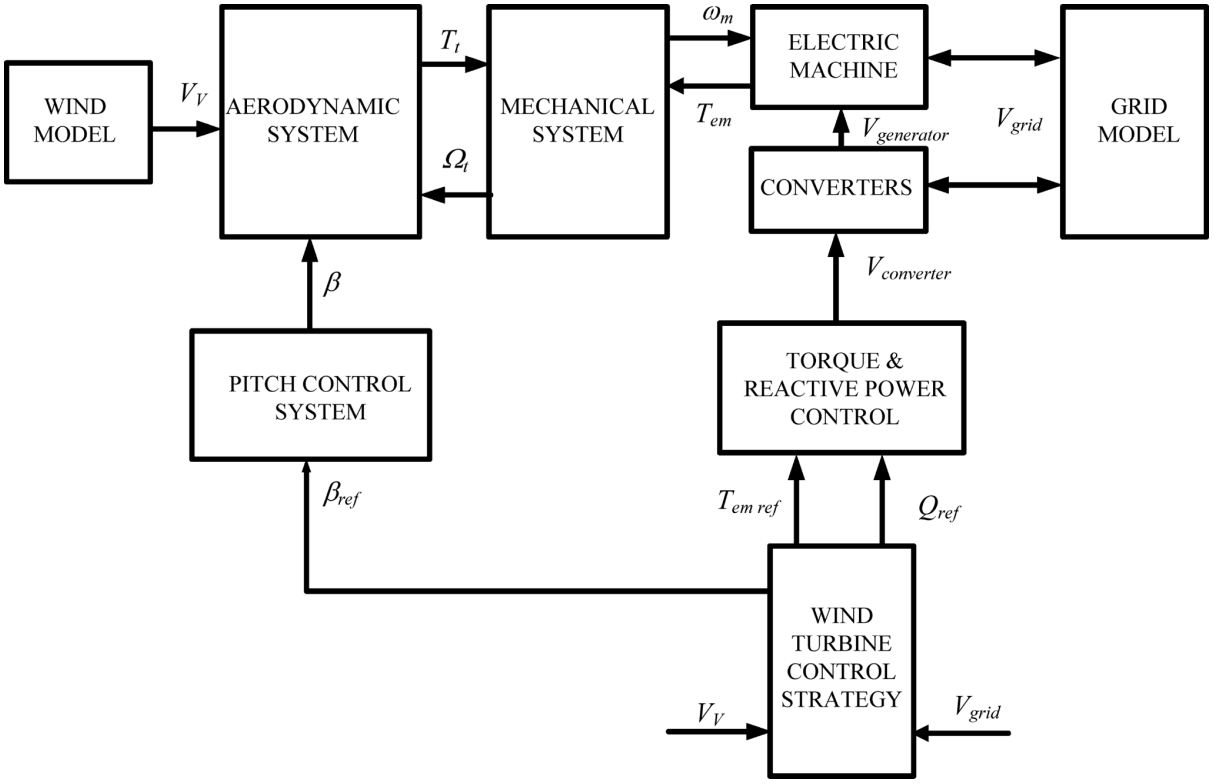

FIGURE 2.6: Block scheme of a variable speed wind turbine model

2.3.1 Aerodynamic Model: The aerodynamic model represents the power extraction of the rotor, calculating the mechanical torque as a function of the airflow on the blades. The torque generated by the rotor has been defined by the following Expression:

$$T_t = \frac{1}{2}\boldsymbol{\pi}\rho R^3 V_v^2 C_t \qquad (2.7)$$

Cp can be measured as a function of tip step ratio (λ) and the pitch angle (β) by one commonly used expression which is easy to adapt to different turbines,

$$C_p = k_1\left(\frac{k_2}{\lambda_i} - k_3\beta - k_4\beta^{k_5} - k_6\right)\left(e^{\frac{k_7}{\lambda_i}}\right) \qquad (2.8)$$

$$\text{Where, } \lambda_i = \frac{1}{\lambda+8}$$

2.3.2 Mechanical System: The mechanical representation of a wind turbine is intricate, involving numerous components and forces. Key dynamics to consider include the resonant frequency of the power transmission train. This train includes

the blades connected to the hub, linked to the slow shaft, which in turn drives the gearbox and fast shaft connected to the generator. focusing on the fundamental resonance frequency of the drivetrain suffices as the second resonance frequency, much higher and lower in magnitude . A two-mass model, depicted in Figure, is suitable for modelling this drive train.

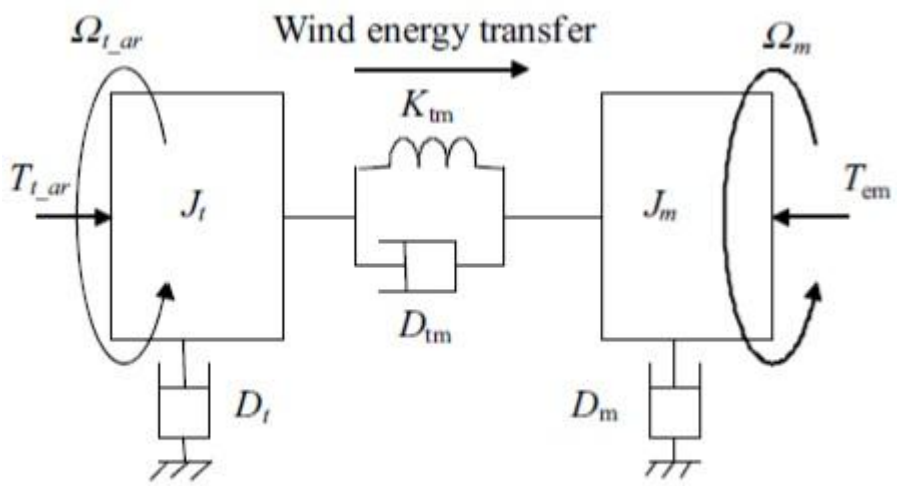

FIGURE 2.7 Two mass mechanical model

Inertia (J_t) relates to turbine-side masses, while (J_m) pertains to the electrical machine's masses. These inertias may overlap if the fundamental resonance originates from the blades.Stiffness (K_{tm}) and damping (D_{tm}) coefficients define the flexible coupling between these inertias, although they do not always directly correspond to the fast shaft.Friction coefficients (D_t) and (D_m) represent mechanical losses due to friction in rotational movement.The turbine's rotational speed and driving torque are expressed within the fast shaft by

$$\Omega_{t\_ar} = N\Omega_t \tag{2.9}$$

$$T_{t\_ar} = \frac{T_t}{N} \tag{2.10}$$

where N is the gearbox ratio. Next,

$$J_t \frac{d\Omega_{t\_ar}}{dt} = T_{t\_ar} - D_t\Omega_{t\_ar} - T_{em}$$

$$J_m \frac{d\Omega_m}{dt} = T_{em} - D_m\Omega_m + T_{em}$$

$$\frac{dT_{em}}{dt} = K_{tm}(\Omega_{t\_ar} - \Omega_m) + D_{tm}\left(\frac{d\Omega_{t\_ar}}{dt} - \frac{d\Omega_m}{dt}\right) \tag{2.11}$$

The model can be simplified by neglecting the damping coefficients (D_t, D_m, and D_{tm}), resulting in a model with two inertias (J_t and J_m) and the stiffness (K_{tm}). The resulting transfer function relating the generator torque and speed presents a pole at ω_{01} pulsation and a zero at ω_{02} pulsation.

$$\omega_{01} = \sqrt{K_{tm}\frac{J_t+J_m}{J_tJ_m}} \tag{2.12}$$

$$\omega_{02} = \sqrt{\frac{K_{tm}}{J_t}} \tag{2.13}$$

2.3.3 Pitch System: The controller is designed for rotating all the blades at the same angle or each of them independently, offering more flexibility and potentially reducing blade stress.When regulating rotational speed around the blades' longitudinal axis, the bandwidth is significantly greater than controlling the angle itself.As a result, a common approach involves representing the control loop, the pitch angle rate of change, and a first-order linear system that captures the primary dynamics of the actuator (whether hydraulic or electric).Figure below shows the block diagram of the blade pitch angle controller.

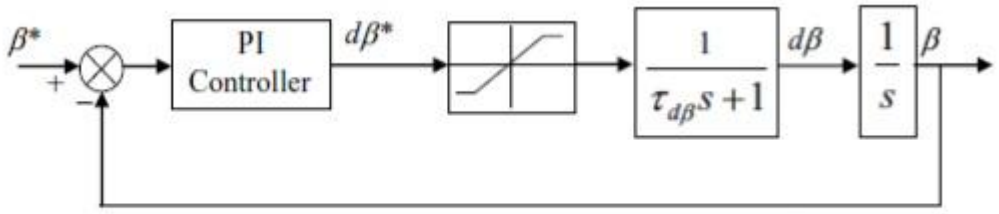

FIGURE 2.8: Pitch control model

2.3.4 Electrical Energy and Converter: Electrical machines are mainly run by power electronic converters. Mainly Doubly Fed Induction Generators and Permanent Magnet Synchronous Generators are used in modern day variable speed wind turbines.

2.3.5 Speed Controller: This controller maintains the generator speed at a specific value for tracking the maximum power. It also generates the reference active power (P_{ref}) for the generator. The wind turbine speed control strategy is illustrated in Fig below. It is classified into four zones.

Zone 1 limits the minimum speed of operation. The generator starts to run at cut in wind speed with a rotating speed Ωm_min .

Zone 2 is used to follow the maximum power extraction at variable speed with respect to a load. With the increase in wind speed, the speed of rotation also 46 gets enhanced until the maximum speed of rotation Ωm_max is reached.

Zone 3 and limits the maximum speed at parallel operation. The energy captured at higher wind speed is regulated at this nominal value.

Zone 4 corresponds to the full load operation and limits the maximum operating speed at rated power output.

The mechanical power is controlled by varying the pitch angle control or by torque control. The electromagnetic torque (τ) is controlled at nominal speed through torque control and the pitch angle is adjusted to keep the turbine at maximum speed and rated power.

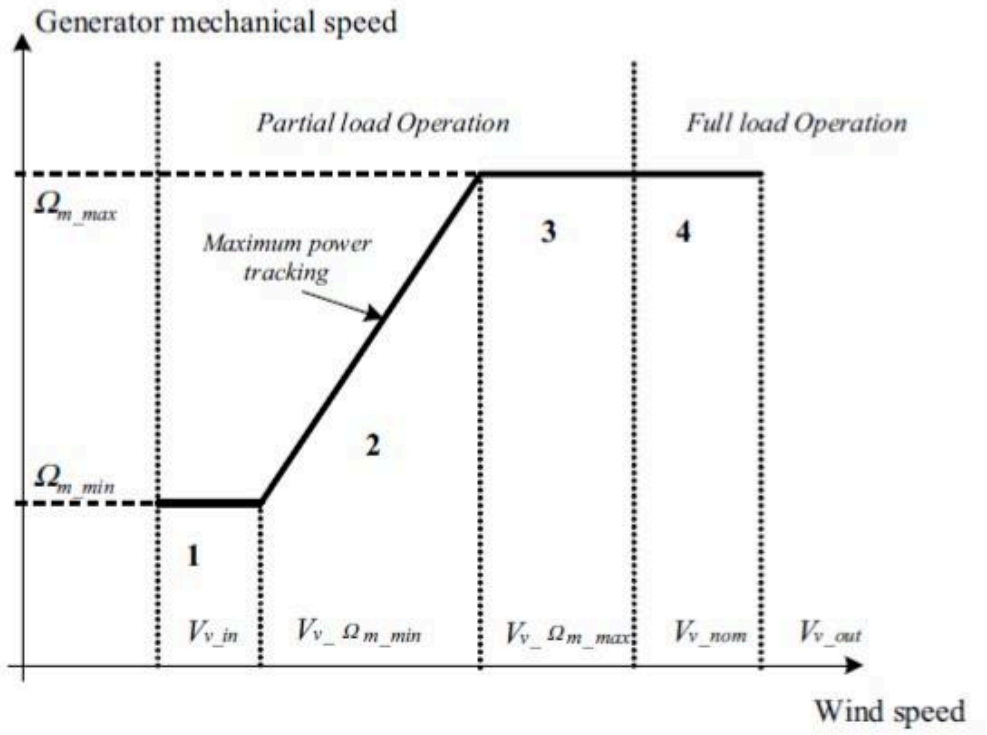

FIGURE 2.9 Operating zones of wind turbine

The figure shows the power versus wind speed characteristics of a wind turbine. We don't prefer to operate the turbine at a very low wind speed (Region 1). The cut-in speed is the wind speed above which the turbine operates. We also have a parameter called cut-out speed, when the wind speed is above cut-out speed the turbine does not work since a phenomenon called Gusting may damage the blades of the turbine. So We prefer to operate the wind turbine at a wind speed in regions 2 and 3.

Now we shall discuss the power versus rotational speed characteristics of a power turbine for different wind speeds. Here it must be noted that the rotational speed of the turbine and the wind speed have no direct relationship. The figure below shows the characteristics.

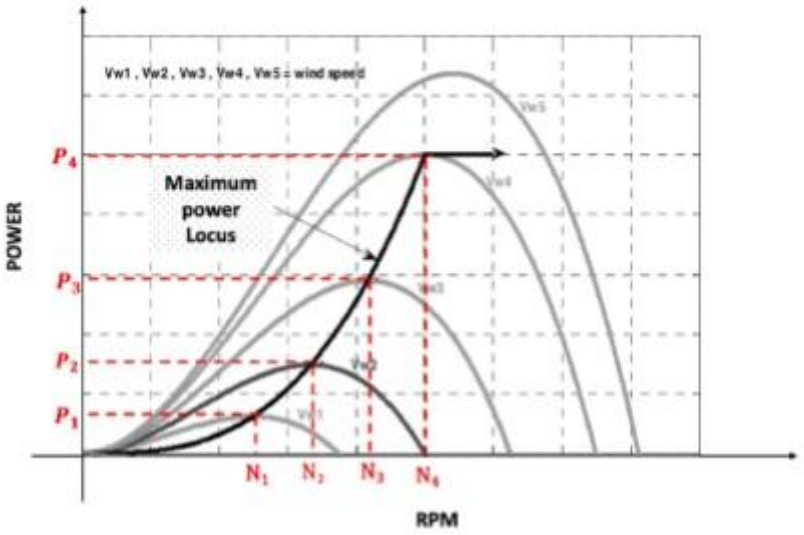

FIGURE 2.9: Power curves at various wind speeds

Our objective is to obtain maximum power for any possible wind speed. accordingly we can form the locus of the maximum power as shown in the figure. The different maximum power for the different wind speed (VW1 <VW2 < VW3 < VW4) along the maximum power locus are represented by P1 ,P2 ,P3 ,P4 and the corresponding rpm of the wind turbine are represented by N1, N2, N3 ,N4 respectively.

2.4 TYPE 3 DFIG BASED VSWT:

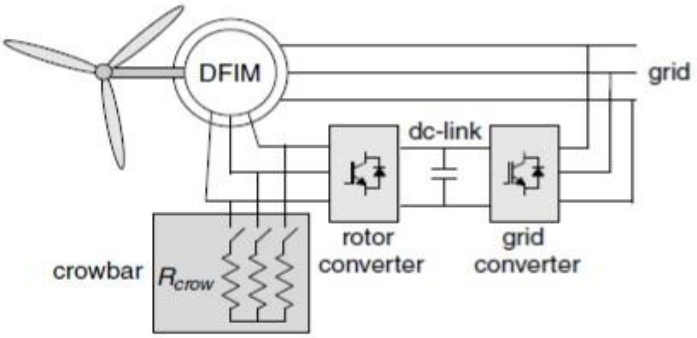

FIGURE 2.10: System equipped with a crowbar

As shown in Figure, the stator circuit is directly connected to the grid. The rotor side and grid side converters respectively rectify the grid voltage and convert it into AC voltage which is given as an excitation to the rotor.

As the wind turbines rotate, they exert mechanical force on the rotor, causing it to rotate. As the rotor rotates the magnetic field produced due to the ac current also rotates at a speed proportional to the frequency of the ac signal applied to the rotor windings. As a result a constantly rotating magnetic flux passes through the stator

windings which cause induction of ac current in the stator winding. Thus the speed of rotation of the stator magnetic field depends on the rotor speed as well as the frequency of the ac current fed to the rotor windings.The frequency of the rotor ac signal increases as the rotor speed decreases and is of positive polarity and vice versa. Thus the frequency of rotor signal should be adjusted such the stator signal frequency is equal to the grid frequency. This is done by adjusting the phase sequence of the rotor windings such that the rotor magnetic field is in the same direction as the generator rotor (in case of decreasing rotor speed) or in opposite direction as the generator rotor (in case of increasing rotor speed).

The use of DFIG based wind turbines has proved to be very successful in power generation. DFIG is a traditional Wound Rotor Induction Generator along with power electronic converters which are externally connected to the stator and rotor.

CHAPTER 3

ANALYSIS OF DOUBLY FED INDUCTION GENERATOR

3.1 INTRODUCTION:

A Doubly Fed Induction Generator (DFIG) is a type of electric generator commonly used in wind turbine systems to convert mechanical energy from the wind into electrical energy that can be fed into the grid. It's a variation of the traditional induction generator that allows for greater control over its output and better performance in variable-speed wind energy conversion systems.Their variable-speed operation and reactive power control capabilities make them well-suited for harnessing energy from varying wind conditions.DFIGs can contribute to grid stability by providing reactive power support and participating in grid control mechanisms. They are used to enhance the integration of renewable energy sources into the existing power grid.

3.2 CONSTRUCTION OF DFIG:

A Doubly Fed Induction generator as its name suggests is a 3 phase wound rotor induction generator where both the rotor and stator windings are fed with 3 phase AC signal. It consists of multi-phase windings placed on both the rotor and stator bodies. The rotor is wound for the same number of poles as that of the stator.
For a 3 phase induction machine the rotor must have 6 terminals that is 2 terminals for each phase, and then the terminals are electrically shorted and connected to slip rings.(the terminals must be internally connected in such a way so that the star or delta connection can be achieved and then the terminals are connected to the 3 slip rings which are further externally connected with brushes).
The main disadvantage with such a wound rotor machine is that the complicated structure of slip rings and brushes must be brought out to the terminals.

3.3 WORKING PRINCIPLE OF DFIG:

Unlike a traditional induction generator, where the rotor windings are short-circuited and not externally connected, the DFIG's rotor windings are connected to the power system through slip rings and brushes. A voltage with frequency same as slip

frequency can be applied at the rotor terminals of the DFIG. Here Our objective is to match the characteristics of the generator with the characteristics of the wind turbine.The following figure shows the torque slip characteristics of a dfig.

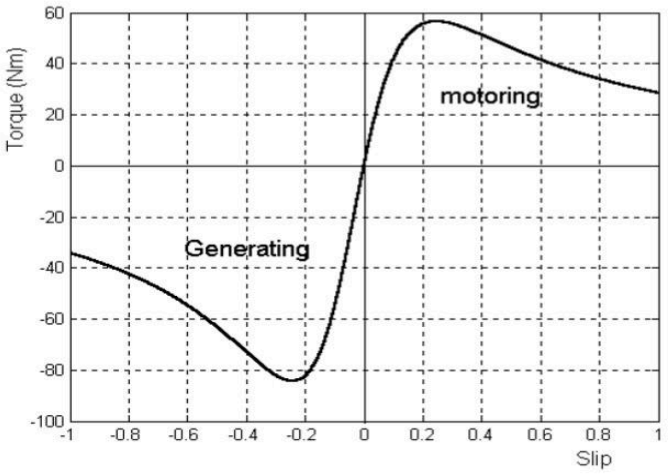

FIGURE 3.1: Torque slip Characteristics of a DFIG

As can be seen in the figure, for the same magnitude of slip, the peak electromagnetic torque developed by the induction machine in the generating region is higher than that of the motoring region. Hence in the generating region the induction machine operates at a lower magnitude of slip than the corresponding motoring region for the same magnitude of electromagnetic torque.The stator and rotor active power,reactive power and generator torque are controlled by adjusting the amplitude,phase and frequency of the voltage induced in the rotor.

Let P_m is a shaft mechanical power, P_s is the active power of stator, P_r is the active power of rotor and P_{Loss} is the active power losses (including copper losses). The mechanical power can be expressed as

$$\mathbf{P_m = P_s + P_r + P_{Loss}} \quad (3.1)$$

Depending on the positive or negative values of slip four operating regions of a DFIG may be obtained as follows:

Case 1: *Sub-synchronous motoring*

In the motoring mode of DFIM, the machine delivers mechanical power and receives electric power from the grid. This is known as the slip power regeneration mode of the machine.

$0 < s < 1$; slip is positive

Pg , Pr , Pm are positive

Case 2: *Super-synchronous Motoring*

With the increase in speed,the stator starts to absorb the rotor power for operating as a motor under supersynchronous speeds.

-1 < s < 0 ; slip is negative
Pg , Pm are positive
Pr is negative
(Pm) = (1-s)*Pg is positive, that is Pm is more than Pg

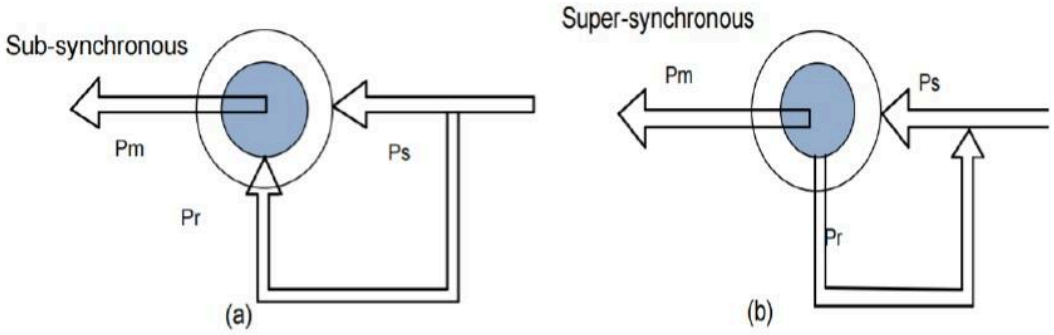

FIGURE 3.3 a) Subsynchronous motoring b) Supersynchronous motoring

speed	Mechanical power developed(P_m)	Stator active power(P_s)	Rotor active power(P_r)
Subsynchronous (s>0)	$P_m>0$	$P_s>0$	$P_r>0$
Supersynchronous (s<0)	$P_m>0$	$P_s>0$	$P_r<0$

Hence a doubly fed machine can perform motoring action even beyond the rated speed.

Case 3: Sub-synchronous Generating
When the machine operates in generating mode at sub synchronous speed, the stator power is absorbed by the rotor.

0 < s < 1 ; slip is positive
P_g , P_r , P_m are negative
(P_m) = (1-s)*P_g is negative, that is P_m is less than P_g

Case 4: Super-synchronous Generating

In generating mode,the rotor delivers a possible recovery power to the Grid.

-1 < s < 0 ; slip is negative
P_g , P_m are negative
P_r is positive
$(P_m) = (1-s)*P_g$ is negative, that is P_m is more than P_g

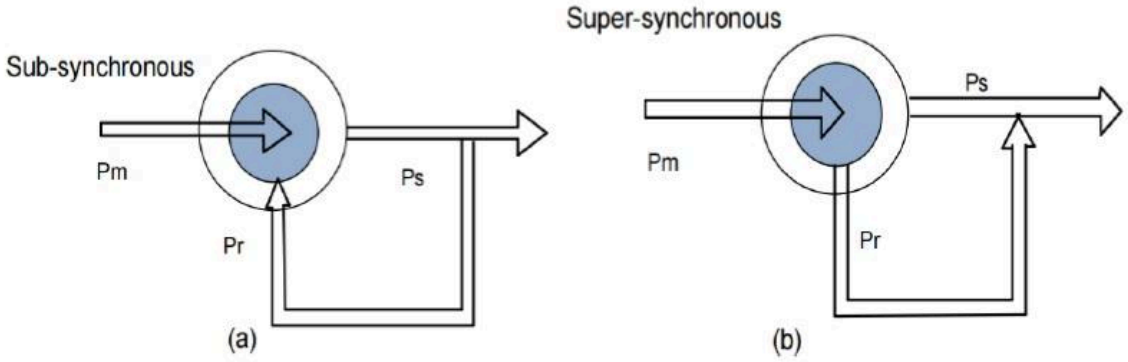

FIGURE 3.4 a) Subsynchronous generating b) Supersynchronous generating

speed	Mechanical power developed(P_m)	Stator active power(P_s)	Rotor active power(P_r)
Subsynchronous (s>0)	$P_m<0$	$P_s<0$	$P_r<0$
Supersynchronous (s<0)	$P_m<0$	$P_s<0$	$P_r>0$

Super synchronous generator case is used in case of a wind turbine, because we get more power at the shaft than the air gap power.

3.4 Steady State Equivalent Circuit:

To represent steady state voltage and current magnitudes, the analysis is carried out using classical phasor theory:

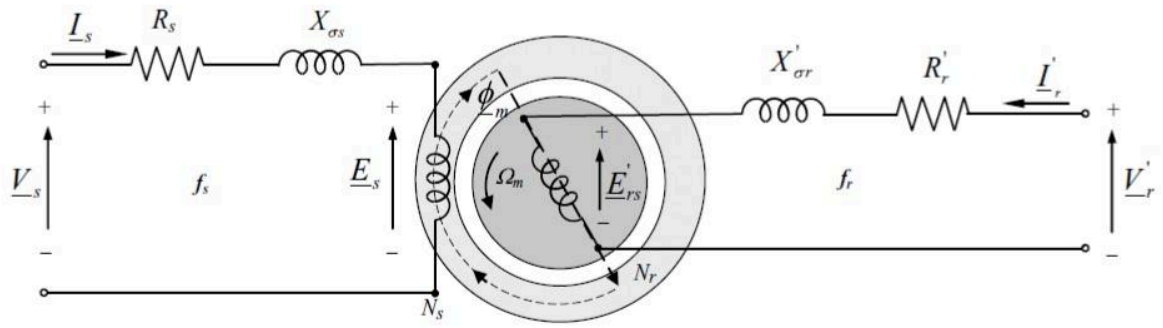

FIGURE 3.5 Single phase equivalent circuit of a DFIG with stator and rotor at different frequencies

Analysing the stator and rotor separately, the steady state model electric equations may be derived as follows.

Stator:

$$\overline{V}_s - \overline{E}_s = (R_s + X_{\sigma s})\overline{I}_s \; at \; f_s \tag{3.2}$$

Where,

$\overline{V}_s$ = supplied stator voltage with frequency f_s (V_{rms})

$\overline{E}_s$ = induced emf in the stator windings with frequency f_s (V_{rms})

$\overline{I}_s$ = induced stator current with frequency f_s (Arms)

$X_{\sigma s} = j.\omega_s.L_{\sigma s}$ = stator leakage impedance (Ω)

Rotor:

$$\overline{V}'_r - \overline{E}'_{rs} = (R'_r + X'_{\sigma r})\overline{I}'_r \; at \; f_r \tag{3.3}$$

Where,

$\overline{E}'_{rs} =$ induced emf in the rotor with frequency f_r, due to the slip between the stator and rotor fields, that is, the induced voltage in the rotor (V_{rms}); later we show that this voltage depends on the speed of the rotor.

$\overline{V}'_r =$ supplied rotor voltage; its frequency should be f_r at steady state, that is, the same frequency as the induced voltage $\overline{E}'_{rs}$ in the rotor (V_{rms})

$\overline{I}'_r =$ induced rotor current with frequency f_r (A_{rms})

$X'_{\sigma r} = j.\omega_r.L'_{\sigma r} = j.s\omega_s.L'_{\sigma r} =$ rotor leakage impedance (Ω);

Rotor side referred to stator: This equivalent circuit is basically similar to an induction machine when the parameters are referred to the stator side. The direction of ir may be feeding into Vr/s or going out from Vr/s;

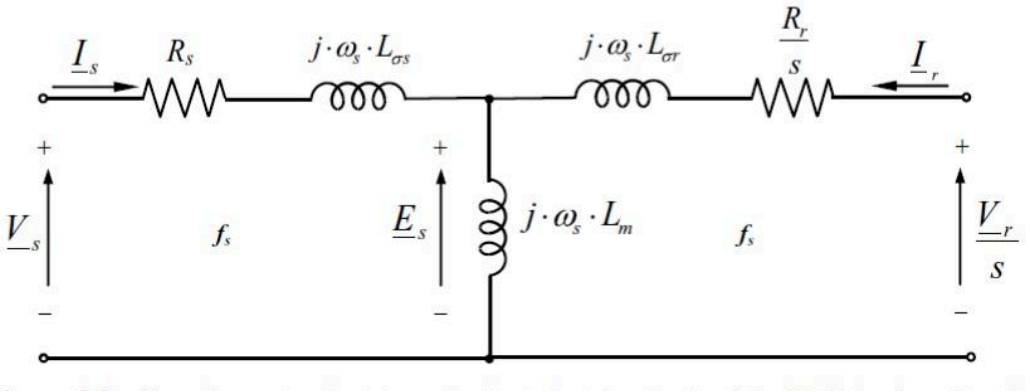

FIGURE 3.6 steady state equivalent circuit of a dfig referred to stator

where L_m is the magnetising inductance of the machine, normally measured at the stator side.

Finally, the equivalent steady state stator referred circuit is derived. The steady state model equation can be represented by combining the stator and rotor equations referred to stator side:

$$\bar{V}_s - \frac{\bar{V}_r}{S} - (R_s + j\omega_s L_{\sigma s})\bar{I}_s + (\frac{R_r}{S} + j\omega_s L_{\sigma s})\bar{I}_r = 0 \ \ at\ f_s \qquad (3.4)$$

Phasor diagram:

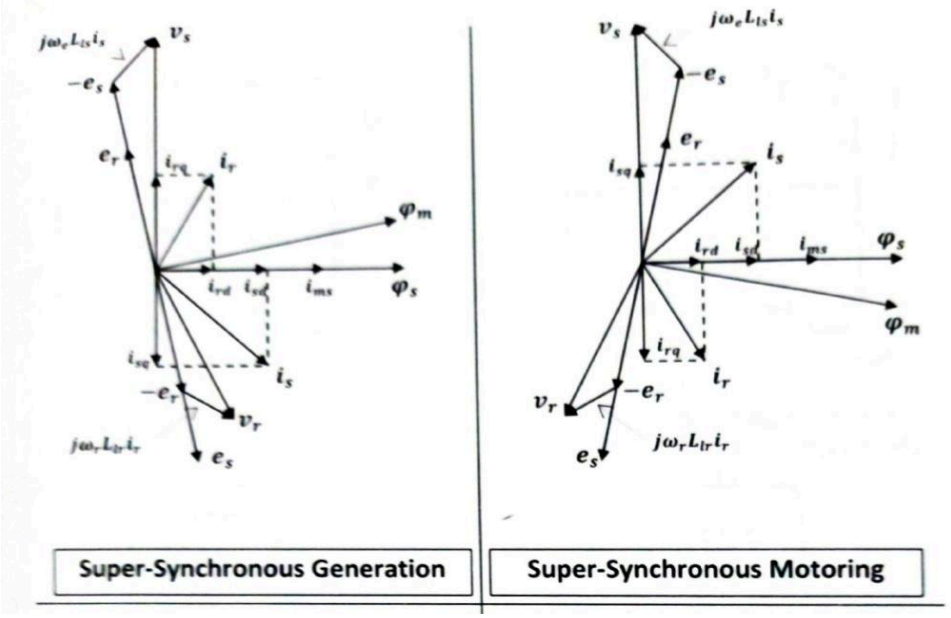

FIGURE 3.7 a) Phasor diagrams of 4 quadrant operation of DFIG

In super synchronous Generation mode stator supply voltage (V_s) lags the air-gap emf ($-e_s$), which indicates extraction of power from stator terminals.But in rotor circuit the angle between rotor back emf (e_r) and rotor current (i_r) is less than 90 degree implying power flow out of rotor circuit.

In super synchronous motoring mode stator supply voltage (V_s) leads the air gap emf ($-e_s$) under all loading conditions, implying power flow into the stator circuit. And the angle between rotor back emf (e_r) and the rotor current is more than 90 degree, implying power flow into the rotor terminals.

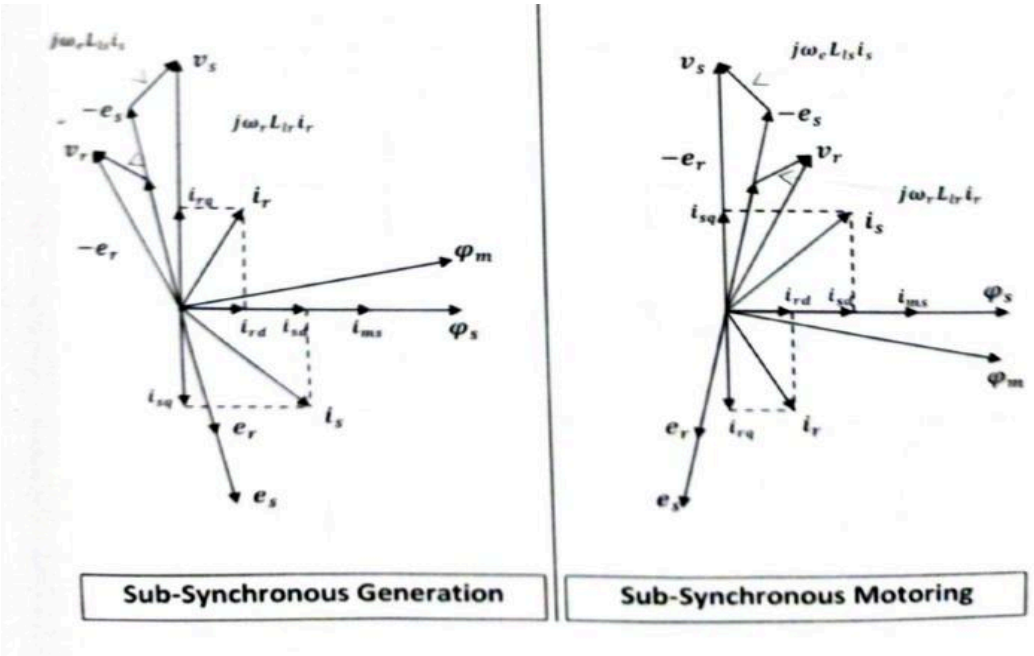

FIGURE 3.7 b) Phasor diagrams of 4 quadrant operation of DFIG

In sub synchronous generation the stator supply voltage (V_s) lags the air gap emf ($-e_s$) which indicates extraction of power from stator terminals.However the angle between rotor back emf (e_r) and rotor current (i_r) exceeds 90 degrees implying power is being fed to the rotor.

In case of super synchronous motoring mode the stator supply voltage leads the air gap emf ($-e_s$) which indicates power is being fed to the stator. However the angle between rotor back emf (e_r) and rotor current is less than 90 degrees which means power is extracted from the rotor circuit.

From the above phasor diagrams it is obvious that:

i) If i_{rd} is suitably controlled, i_{sd} gets automatically adjusted giving optimal stator power factor.

ii) Depending on the positive or negative values of i_{sq}, torque varies taking the machine from generating to motoring mode.

For a DFIG driven by a wind turbine, the aerodynamic torque varies as the wind speed changes. With the interference of the V_r, the Te may be varied so that the generator operates at the required speeds. Meanwhile,regulating the rotor voltage may control the stator side power factor.

3.5 D-Q MODELLING OF DFIG:

The stator and the rotor windings are transformed to their two-phase equivalent using the park or dq0- transformation based on a complex equivalent circuit of DFIG as shown in Fig 3.3.2(c). By using the d-q model, three to two phase representations are described.

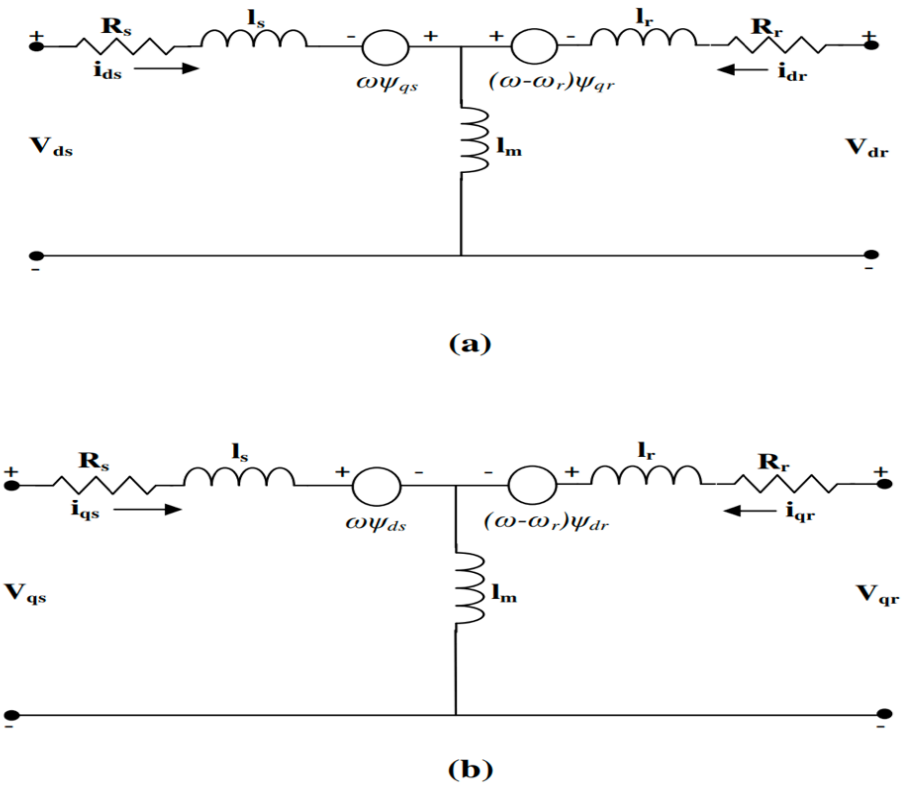

FIGURE 3.8:- Equivalent circuit of DFIG in d-q axis respectively

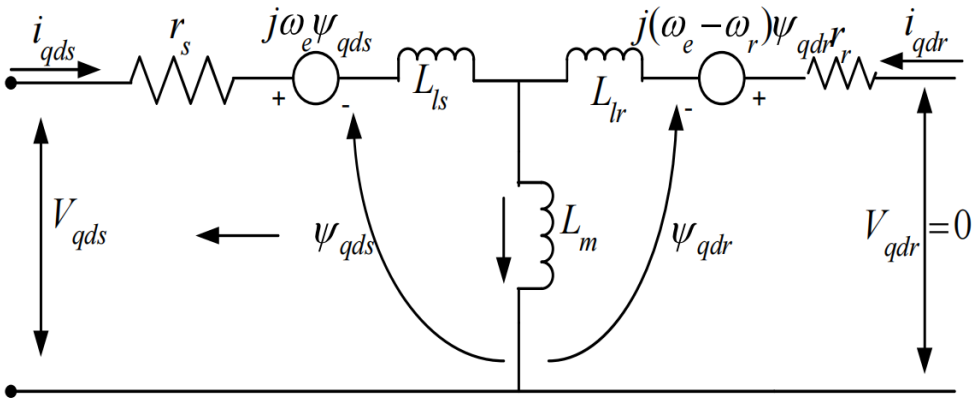

FIGURE 3.9:-overall d-q circuit

The following assumptions are made for developing the d-q model of induction machine :

- Iron losses are neglected.
- Stator and rotor skin effects are neglected.
- Magnetising inductance saturation is neglected.

- Constant air gap reluctance.
- Stator and rotor windings of the DFIG are assumed to be symmetric.
- Windings are assumed as sinusoidally distributed..

The mathematical model according to Park's transformation for the stator and rotor voltage in an arbitrary d-q axis rotating frame with an angular speed we is discussed below:

$$Vds = i_{ds}R_s + \frac{d\varphi_{ds}}{dx} - \omega_e\varphi_{qs} \quad (3.5)$$

$$Vqs = i_{qs}R_s + \frac{d\varphi_{qs}}{dx} + \omega_e\varphi_{ds} \quad (3.6)$$

$$Vdr = i_{dr}R_r + \frac{d\varphi_{dr}}{dx} - \omega_e\varphi_{qr} \quad (3.7)$$

$$Vqr = i_{qr}R_r + \frac{d\varphi_{qr}}{dx} + \omega_e\varphi_{dr} \quad (3.8)$$

Stator and rotor fluxes are magnetically decoupled in d and q axis respectively as follows:

$$\varphi_{ds} = L_s i_{ds} + L_m i_{dr} \quad (3.9)$$

$$\varphi_{qs} = L_s i_{qs} + L_m i_{qr} \quad (3.10)$$

$$\varphi_{dr} = L_r i_{dr} + L_m i_{ds} \quad (3.11)$$

$$\varphi_{qr} = L_r i_{qr} + L_m i_{qs} \quad (3.12)$$

Using equations 3.5 to 3.8, combining d-q axis together to find stator and rotor voltages, we get:

$$V_{dqs} = i_{dqs} * R_s + \frac{d\varphi_{dqs}}{dx} + j\omega_e\varphi_{dqs} \quad (3.13)$$

$$V_{dqr} = i_{dqr} * R_r + \frac{d\varphi_{dqr}}{dx} + j\omega_e\varphi_{dqr} \quad (3.14)$$

$$\varphi_{dqs} = L_s i_{dqs} + L_m i_{dqr} \quad (3.15)$$

$$\varphi_{dqr} = L\ i_{dqr} + L_m i_{dqs} \quad (3.16)$$

Where i_{dqs} and I_{dqr} are the complex conjugates of the stator and rotor current vector. The stator and rotor inductances are given by:

$$L_s = L_{ls} + L_m \quad (3.17)$$

$$L_r = L_{lr} + L_m \quad (3.18)$$

Where Lm is the mutual inductance consequently, Active and Reactive powers on stator and rotor side are defined as:

$$P_s = V_{ds}\ i_{ds} + V_{qs}i_{qs} \quad (3.19)$$

$$Q_s = V_{qs}i_{qs} - V_{ds}i_{ds} \quad (3.20)$$

$$P_r = V_{dr} i_{dr} + V_{qr} i_{qr} \quad (3.21)$$

$$Q_r = V_{qr} i_{qr} - V_{dr} i_{dr} \quad (3.22)$$

In the above equations

V_{ds} , V_{dr} , V_{qs} , V_{qr} , i_{ds} , i_{qs} ,i_{dr} , i_{qr} are the stator and rotor voltages and current in d-q axis reference frame. Suffix d, q denotes axis and suffix s, r denotes stator and rotor values respectively.

$\varphi_{ds}, \varphi_{dr}, \varphi_{qs}, \varphi_{qr}$ represent the stator and rotor fluxes in d-q axis reference frame.

Rs and Rr are the stator and rotor winding resistances

Ls, Lr, Lm are the stator, rotor and mutual inductances.

ω_s is the reference speed which depends upon the supply frequency and the no of poles of the machines, and ω_r is the rotor rotational speed.

Ps, Qs, Pr, Qr are active and reactive power of stator and rotor side of DFIG system.

CHAPTER 4

ANALYSIS OF BACK TO BACK CONVERTER

4.1 INTRODUCTION: The basic requirement for the electricity generation using wind energy is to produce ac signal of constant frequency irrespective of the wind speed. To achieve this, the frequency of ac signal applied to the rotor windings needs to be adjusted. This task is accomplished using a voltage source back to back PWM converter as shown below.

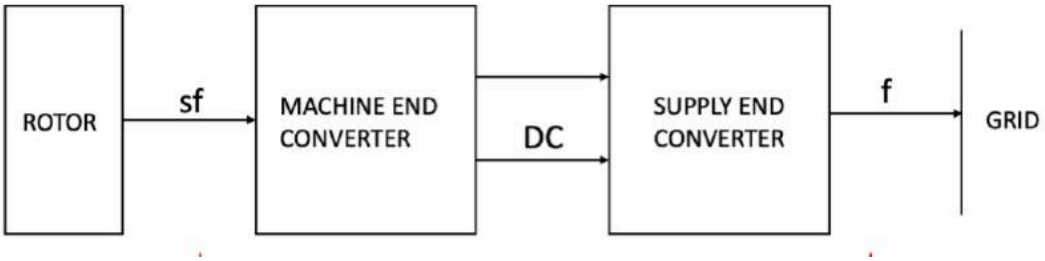

FIGURE 4.1 *Bidirectional converter block*

back-to-back converter is a bi-directional power converter consisting of two conventional pulse width modulation (PWM) voltage source converters and a common DC bus employing a DC link capacitor. Both stator and rotor are able to supply the power, but the direction of active power flow through the rotor circuit is dependent on the wind speed and accordingly the generator speed.

The machine side converter is used to control the active and reactive powers of the stator by controlling the d-q components of the rotor and also torque and speed of the machine,thus enabling variable speed operation.It also generates the voltage applied to the DFIG rotor.

The grid side converter is used to maintain a constant dc link voltage and ensures the unity power factor operation by making the reactive power drawn from the utility grid to zero.

Below the synchronous speed, the active power flows from the grid to the rotor side and the rotor side converter (RSC) acts as voltage source inverter while grid side converter (GSC) acts as a rectifier. Due to the bi-directional power flow ability of the

converter, the DFIG may operate as a generator or motor in both sub synchronously (0<slip<1) and super synchronously (slip<0).The higher the slip, the larger the electrical power,which is either absorbed or delivered through the rotor.

A capacitor is connected between the two converters such that it acts as an energy storage unit(during super synchronous motoring and subsynchronous generating).
This back to back arrangement provides a fixed voltage fixed frequency output irrespective of the variable frequency, variable voltage output of the generator.

The active crowbar function monitors the voltage levels on the rotor-side converter and detects any overvoltage conditions that could potentially damage the converter or other components. If the voltage exceeds a certain threshold, the active crowbar is triggered.When the active crowbar is activated, it provides a low-impedance path for the excessive current to flow. This typically involves short-circuiting the terminals of the rotor-side converter, diverting the overvoltage transient away from sensitive components. Its unavoidable drawback is that the stator would absorb reactive power from the grid.

4.2 GRID SIDE CONVERTER CONTROL: The grid side system is composed by the grid side converter, the grid side filter, and the grid voltage.The grid side converter is modelled with ideal bidirectional switches. It converts voltage and currents from DC to AC, while the exchange of power can be in both directions from AC to DC (rectifier mode) and from DC to AC (inverter mode). The ideal switch normally is created by a controlled semiconductor with a diode in antiparallel to allow the flow of current in both directions. In this exposition, the controlled semiconductor used is an insulated gate bipolar transistor (IGBT).

The objective of the supply-side converter is to keep the dc-link voltage constant regardless of the magnitude and direction of the rotor power. A vector-control approach is used with a reference frame oriented along the stator (i.e. supply) voltage vector position. This enables independent control of the active and reactive power flowing between the supply and the GSC. The PWM converter is current regulated, with the direct axis current used to regulate the dc-link voltage and the quadrature axis current component used to regulate the reactive power.

The dc-link voltage can be controlled via iq. The control scheme thus utilises current control loops for id and iq, with the id demand being derived from the dc-link voltage error through a standard PI controller. The iq demand determines the displacement factor on the supply-side of the inductors. The strategy is shown in Fig.4.2.

Active and reactive power flow in dq frame is given as follows,

$$P = 3(V_d i_d + V_q i_q) \quad (4.1)$$

$$Q = 3(V_d i_q + V_q i_d) \quad (4.2)$$

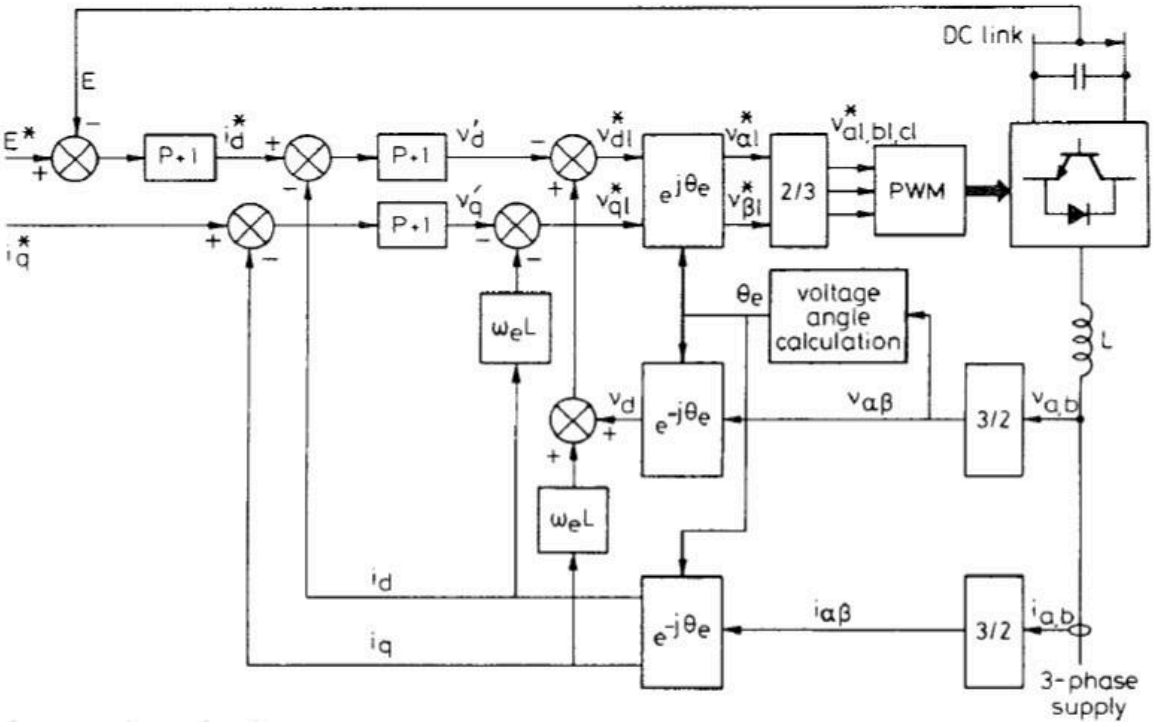

FIGURE 4.2 *Grid side converter control*

The angular position of the supply voltage vector is calculated as follows,

$$\theta_e = \int \omega_e dt = tan^{-1}(\frac{v_\beta}{v_\alpha}) \quad (4.3)$$

Where v_α and v_β are the α, β (stationary 2-axis) stator voltage components.
Aligning the d-axis of the reference frame along the stator-voltage position results in the active and reactive powers to be proportional to d and q axis currents respectively.

the reference voltages are given by,

$$v^*_{d1} = -v'_d + (\omega_e L i_q + v_d) \quad (4.4)$$

$$v^*_{q1} = -v'_q - \omega_e L i_d \quad (4.5)$$

4.3 ROTOR SIDE CONVERTER CONTROL: The induction machine is controlled in a synchronously rotating dq axis frame, with the d-axis oriented along the stator-flux vector position. This gives rise to a decoupled control of the electrical torque and the rotor excitation current is obtained. The rotor-side PWM converter provides the actuation, and the control requires the measurement of the rotor and stator currents, stator voltage and the rotor position.

Under the stator-flux orientation, the relationship between torque and dq axes voltages, currents and fluxes can be written as;

$$\lambda_s = \lambda_{ds} = L_0 i_{ms} = L_s i_{ds} + L_0 i_{dr} \quad (4.6)$$

$$\lambda_{dr} = \frac{L_0^2}{L_s} i_{ms} + \sigma L_r i_{dr} \quad (4.7)$$

$$\lambda_{qr} = \sigma L_r i_{qr} \quad (4.8)$$

$$i_{qs} = -\frac{L_0}{L_s} i_{qr} \quad (4.9)$$

$$v_{dr} = R_r i_{dr} + \sigma L_r \frac{di_{dr}}{dt} - \omega_{slip} \sigma L_r i_{qr} \quad (4.10)$$

$$v_{qr} = R_r i_{qr} + \sigma L_r \frac{di_{qr}}{dt} + \omega_{slip} (L_m i_{ms} + \sigma L_r i_{dr}) \quad (4.11)$$

$$T_e = -3\frac{P}{2} L_m i_{ms} i_{qr} \quad (4.12)$$

$$\omega_{slip} = \omega_e - \omega_r \quad (4.13)$$

$$\sigma = 1 - \frac{L_0^2}{L_s L_r} \quad (4.14)$$

$$L_m = \frac{L_0^2}{L_s} \quad (4.15)$$

The stator flux angle is calculated from,

$$\lambda_{\alpha s} = \int (v_{\alpha s} - R_s i_{\alpha s}) dt \quad (4.16)$$

$$\lambda_{\beta s} = \int (v_{\beta s} - R_s i_{\beta s}) dt \quad (4.17)$$

$$\theta_s = tan^{-1}\left(\frac{\lambda_{\beta s}}{\lambda_{\alpha s}}\right) \quad (4.18)$$

Where the above angle gives the position of the stator-flux position. The torque is proportional to i_{qr} and can be regulated using v_{qr}. The rotor excitation current idr is controlled using v_{dr}. Assuming that all reactive power to the machine is supplied by the stator, the reference idr may set to zero.

The figure shows the schematic of the RSC control. The q-axis rotor current can be obtained either from a outer speed control loop or from a reference torque imposed on the machine. These two options may be termed as speed-control mode or torque-control mode for the generator.

An analysis of the rotor circuit similar to that done for the grid-side converter results in the following voltage equations,

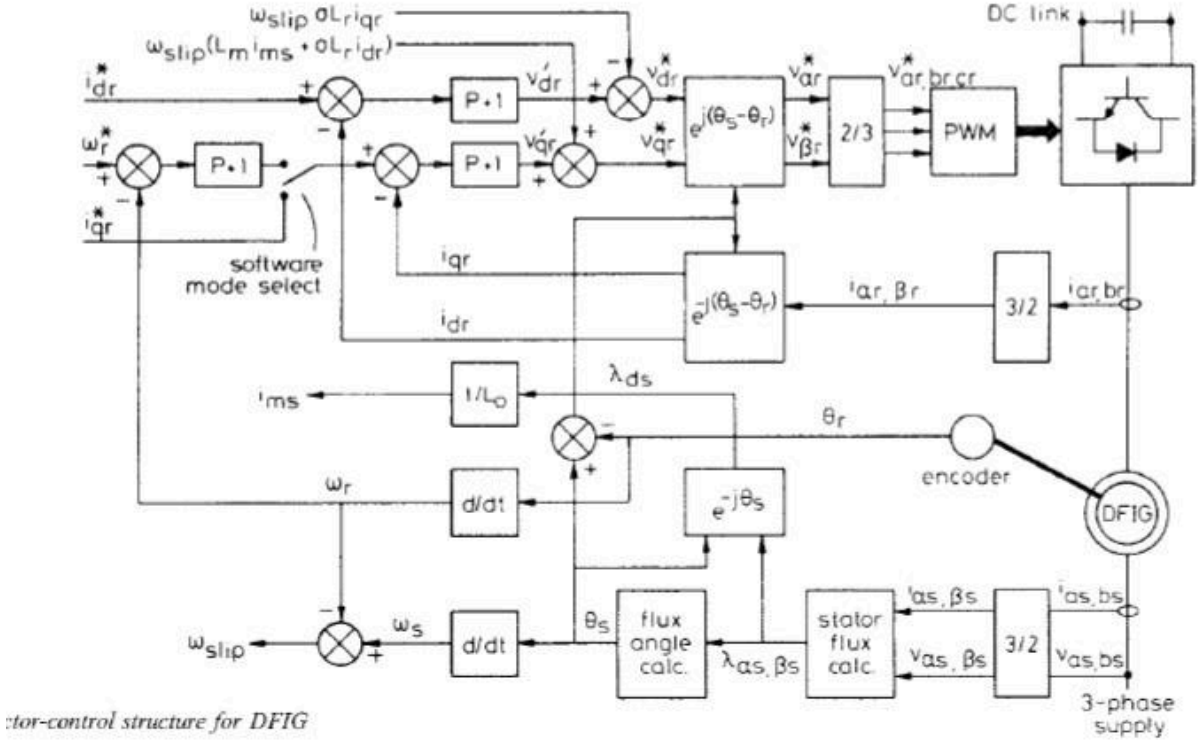

:tor-control structure for DFIG

FIGURE 4.3 *Rotor side converter control*

The reference q-axis rotor current can be obtained either from a outer speed-control loop or from a reference torque imposed on the machine. These two options may be termed a speed-control mode or torque-control mode for the generator. A similar analysis for the control of the dq currents carried out for the supply-side converter can likewise be done for the control of the dq rotor machine currents. From the rotor-voltage equation in eqn. 11 we have

$$V_{dr}^{'} = R_r i_{dr} + \sigma L_r \frac{di_{dr}}{dt} \quad (4.19)$$

$$v_{qr}^{'} = R_r i_{qr} + \sigma L_r \frac{di_{qr}}{dt} \quad (4.20)$$

The i_{dr} and i_{qr} errors are processed by the PI controller to give V_{dr}, and v_{qr}, respectively. To ensure good tracking of these currents, compensation terms are added to v_{dr} and v_{qr}, to obtain the reference voltages v_{dr}^{*} and v_{qr}^{*} according to

$$v_{dr}^{*} = -v_{dr}^{'} - \omega_{slip}\sigma L_r i_{qr} \quad (4.21)$$

$$v_{qr}^{*} = v_{qr}^{'} + \omega_{slip}(L_m i_{ms} + \sigma L_r i_{dr}) \quad (4.22)$$

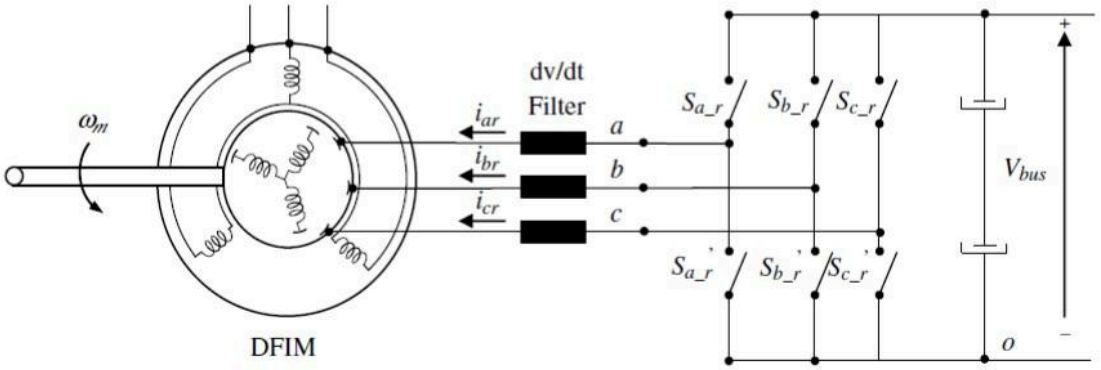

FIGURE 4.4 *DFIM with grid filters and converter*

Between the rotor and the converter, in general, a dv/dt filter is located mainly with the objective to protect the machine from the harmful effects of the voltage source converter, such as capacitive leakage currents, bearing currents, and increased stress on the motor insulation.The rotor side converter is connected to the grid side converter by the DC link.

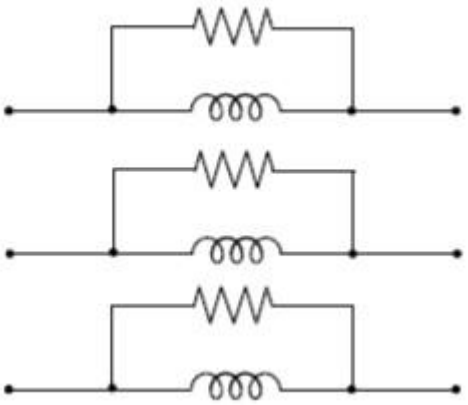

FIGURE 4.5 The dv/dt filter at the output of the converter.

The dv/dt filter mainly tries to attenuate the step voltages in the rotor terminals of the machine, coming from the converter. The combination of mainly three factors determine how harmful the effects are on the machine, which the dv/dt filter tends to mitigate. These factors are the type of voltage steps generated by the converter, the

characteristics and length of cable used for connecting the converter and the machine, and finally the characteristics of the machine that is being supplied. The attenuation of the step voltages can be achieved, in general, by different types of filters.Therefore, one possible solution to attenuate the overvoltages at the terminals of the motor is to locate a resistance and an inductance in parallel at the output of the converter. The resistance damps the reflection in the cable, while the inductance is necessary to reduce the voltage drop and the losses due to low frequencies.

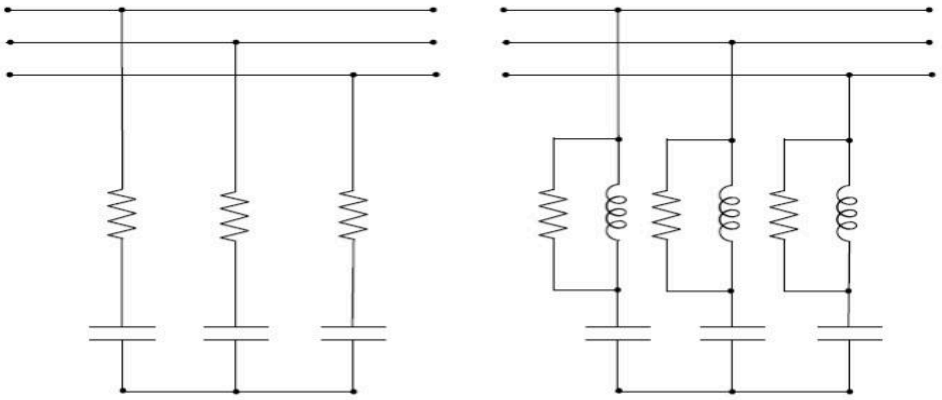

FIGURE 4.6 *dv/dt filter topology*

Filters whose objective is to couple the input impedance of the motor with the impedance of the cable are normally located at the terminals of the motor. Among different solutions, it is possible to locate an RC or an RLC filter, as shown in Figure.Finally, at the output of the converter it is also possible to locate filter networks, as
shown in Figure 4.5, to reduce the dv/dt at the converter itself. Hence, the effect that produces the inclusion of a dv/dt filter is graphically depicted in Figure. It is possible to see how, without the filter, the overvoltage that occurs at the terminals of the motor is quite significant, while thanks to the inclusion of the proper filter this overvoltage is reduced.
The DC part of the back-to-back converter is typically called the DC link. Thanks to the energy stored in a capacitor (or combination of several capacitors), it tries to maintain a constant voltage in its terminals. It is the linkage between the grid side and rotor side converters. It is composed of a capacitor in parallel with a high resistance.

CHAPTER 5

VOLTAGE DIP ANALYSIS

5.1 INTRODUCTION: If a defined fault occurs on the transmission system, it is a normal requirement of the transmission system operator that a generating station remain in operation and connected to the system—thus, it "rides through" the fault. This issue is very important for the grid integration of wind energy systems.Voltage dips are primarily caused by short duration overcurrents flowing through the power system. The principal contributions to overcurrents are power system faults, motor starting, and transformer energising.

A network fault indicates either a short-circuit condition or an abnormal open-circuit condition. The nature of voltage dips can be influenced by the symmetry of a network Fault. A voltage dip causes overcurrents and overvoltages in the rotor windings, which would damage the converter connected to their terminals if no counter measures were taken.

The voltage dips occurring at the machine terminal may be symmetrical or asymmetrical; However as the first step towards the objective of this thesis we will concentrate only on the symmetrical voltage dip analysis.

5.2 EMF INDUCED IN THE ROTOR: From the point of view of the rotor converter, the electromagnetic force is one of the most important variables, since it acts as a perturbation in the control loops. The electromagnetic force induced in the rotor windings varies considerably under grid disturbances. This is the cause of the problematic behaviour of DFIMs under perturbations as it could saturate the converter.

We rewrite the rotor voltage expression as,

$$\overline{V}_r^r = R_r \overline{i}_r^r + \frac{d}{dt}\overline{\psi}_r^r \tag{5.1a}$$

The stator and rotor fluxes are related as,

$$\overline{\psi}_r^r = \frac{L_m}{L_s}\overline{\psi}_s^r + \sigma L_r \overline{i}_r^r \tag{5.1b}$$

Where $\sigma = 1 - \frac{L_m^2}{L_s L_r}$ is the leakage coefficient.

Combining Equations (6.1a) and (6.1b), the following expression is obtained,

$$\overline{V}_r^r = \frac{L_m}{L_s}\frac{d}{dt}\overline{\psi}_s^r + (R_r + \sigma L_r \frac{d}{dt})\,\overline{i}_r^r \tag{5.2}$$

Thus, the rotor voltage might be divided into two terms. The first term corresponds to

the emf induced by the stator flux in the rotor. It is the voltage in the rotor open-circuit terminals (where i_r=0).The second term only appears if there is a current in the rotor. It is due to the voltage drop in both the rotor resistance R_r and the rotor transient inductance, σL_r.

The expression for the first term is,

$$\overline{e_r^r} = \frac{L_m}{L_s}\frac{d}{d}\overline{\psi_s^r} \tag{5.3}$$

Or, if the variables are expressed in a stator reference frame, we have,

$$\overline{e_r^s} = \frac{L_m}{L_s}\left(\frac{d}{dt}\overline{\psi_s^s} - j\omega_m\overline{\psi_s^s}\right) \tag{5.4}$$

During normal operation, the electrical grid is a source of three balanced voltages of constant amplitude and frequency. That is, the three phases have the same voltage and are shifted 120°.Thus, the space vector of the stator voltage is a rotating vector of constant amplitude $\overline{V_g}$ that rotates at synchronous speed ω_s:

$$\overline{V_s^s} = \overline{V_g}e^{j\varphi}e^{j\omega_s t} = \sqrt{2}\overline{V_g}e^{j\omega_s t} \tag{5.5}$$

The phasor of the stator flux is found to be,

$$\overline{\psi_s} = \frac{\overline{V_g}}{j\omega_s} \tag{5.6}$$

So, at steady state, the space vector of the stator flux is a rotating vector of constant amplitude, proportional to the grid voltage, and synchronous speed:

$$\overline{\psi_s^s} = \frac{\overline{V_g}}{j\omega_s}e^{j\varphi}e^{j\omega_s t} \tag{5.7}$$

From the point of view of the rotor windings, the rotational speed of the stator flux is the difference between the synchronous speed and the electrical rotor speed; that is, the slip frequency. Thus the flux across the rotor is variable, as seen if it is expressed in a rotor reference frame:

$$\overline{\psi_s^r} = \sqrt{2}\overline{\psi_s}e^{j\omega_r t} \tag{5.8}$$

This variable flux will thus induce an emf proportional to the slip frequency:

$$\overline{e_r^r} = \frac{L_m}{L_s}\frac{d}{dt}\overline{\psi_s^r} = j\omega_r\frac{L_m}{L_s}\overline{\psi_s^r} \tag{5.9}$$

The amplitude of this emf can be expressed as a function of the stator voltage:

$$\left|\overline{E_r}\right| = \omega_r\frac{L_m}{L_s}\frac{V_g}{\omega_s} = \overline{V_g}\frac{L_m}{L_s}s \tag{5.10}$$

5.3THREE PHASE VOLTAGE DIPS: A voltage dip refers to an abrupt reduction in one or more voltage phases. When this drop is identical across all three phases, it is termed a three-phase, symmetrical, or balanced dip. Such a fault can occur due to factors like inrush currents during motor start-up or a nearby short-circuit involving all three phases and the ground.

If the the voltage drops at time t=0 from its initial prefault voltage to 0 value then it is called as total voltage dip.It is often assumed that when the stator is without voltage, the machine becomes demagnetized, meaning there is no magnetic flux and consequently no electromotive force (emf) induced in the rotor windings. In fact, it is true that, in the steady state, the flux is proportional to the stator voltage, and therefore if the dip is long enough, the machine will demagnetize completely. jHowever, the flux cannot be discontinuous as it is a state variable. On the contrary, the flux evolves from its initial value prefault to zero, resulting in a transient emf induced in the rotor terminals.

The evolution of the stator flux can be calculated mathematically from the dynamic expression of the stator, With the rotor under total voltage dip,

$$\frac{d}{dt}\overline{\psi_s^s} = -\frac{R_s}{L_s}\overline{\psi_s^s} \quad (5.11)$$

the solution of expression is:

$$\overline{\psi_s^s} = \overline{\psi_0} e^{-t/\tau_s} \quad (5.12)$$

where $\overline{\psi_0}$ is the initial value of the flux (for t=0) and $\tau_s = \frac{L_s}{R_s}$ is the time constant of the stator.

The value of $\overline{\psi_0}$ can be calculated by considering the flux just before and after the dip appearance.As the flux must be continuous, both expressions must yield the same value at t=0. Consequently, we have

$$\overline{\psi_0} = \frac{\widehat{V}_{pre}}{j\omega_s} \quad (5.13)$$

One important characteristic of the flux during the dip is that it doesn't rotate: it is fixed with the stator. In other words, the flux, which was rotating at the grid frequency before the dip, freezes during the dip. Its amplitude decays exponentially from its initial value to zero with the time constant of the stator.grid. This transitory flux induces an emf in the rotor windings. However as this transitory flux is static from rotor frame of reference it appears to be rotating at a much higher speed (ω_r) as compared to the steady state flux (slip speed).Consequently, the emf induced by the transitory flux will be much higher than the emf induced by the steady state during normal operation. The maximum voltage is induced at the beginning of the dip can be calculated as,

$$\left|E_{r,max}\right| \approx \frac{L_m}{L_s}\frac{\omega_m}{\omega_s}\widehat{V_{pre}} = \widehat{V_{pre}}\frac{L_m}{L_s}(1-s) \qquad (5.14)$$

It can be deduced that, in the case of a voltage dip, the amplitude of the emf induced at the beginning of a total dip can be 3 to 5 times higher than during normal operation. This abnormal overvoltage in the rotor notably affects the operation of the rotor converter, usually saturating the converter and resulting therefore in the loss of current control.

5.4 PROPOSED PROTECTION SCHEME UNDER TOTAL VOLTAGE DIP:

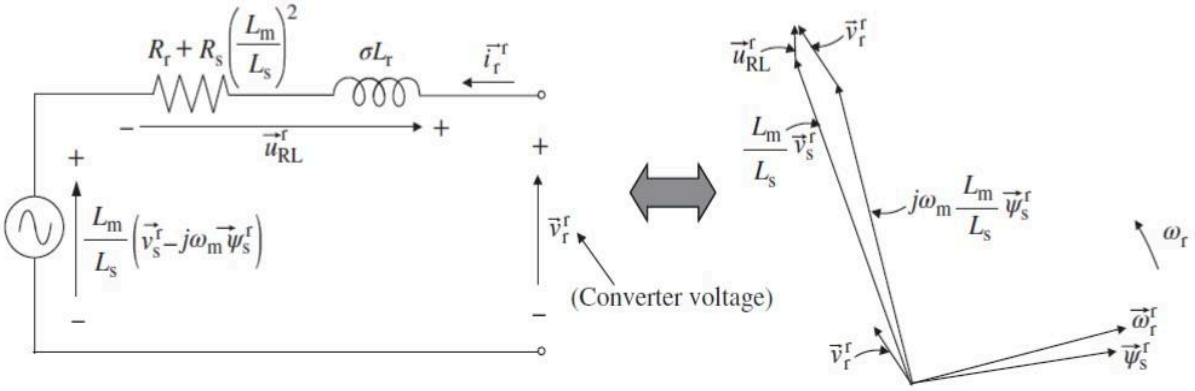

Figure 5.1 (a) *Equivalent circuit of the DFIM for the analysis of voltage dips* **5.1** ***(b)*** *space vector diagram at sub synchronism in a generator mode*

The above mentioned phasor diagram is observed under steady state.But under a voltage dip, the stator voltage ($\frac{L_m}{L_s}[\overline{V_s^r}]$) suddenly reduces to a much smaller value. However the stator flux ($j\omega_m[\frac{L_m}{L_s}]\ \overline{\psi_s^r}$) can't evolve rapidly. Now, as the rotor current

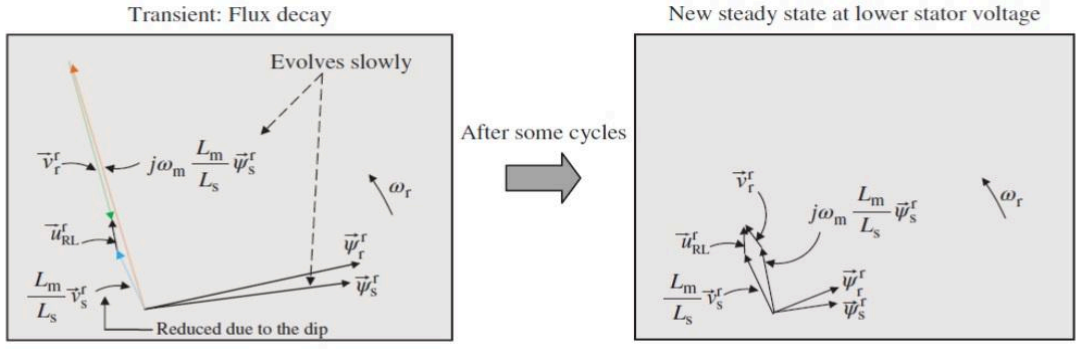

Figure 5.2 *Evolution of the space vector magnitudes from the first instant when the stator voltage is reduced until the steady state reached at the dip*

Is an image of the rotor induced voltage, ($\overline{U_{RL}^r}$) a very large converter voltage ($\overline{V_r^r}$) is required to maintain a fixed rotor voltage under voltage dips.However the

back-to-back converters are not dimensioned to handle such large voltages,so we lose control under such voltage dips.

Generally, because of this voltage limitation, wind turbines based on DFIM incorporate an additional crowbar protection that solves these problematic severe voltage dips.Therefore, it can be concluded that after a severe voltage dip, during the time the stator flux evolves, there is typically a short period when control is lost, which normally produces overcurrents at the stator and rotor of the machine, until the flux reaches one level at which the available converter voltage can guarantee the Control of the machine. As said before, in order to protect the system against the overcurrents provoked by the loss of control, a crowbar protection is activated that simultaneously accelerates the flux evolution, while trying as quickly as possible, to recover control with the converter.Whenever voltage dip arises the high rotor current

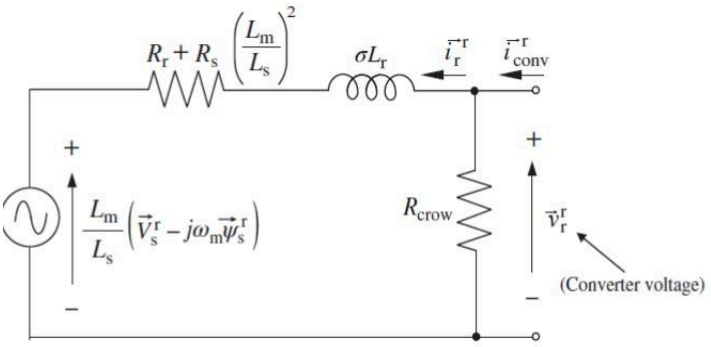

(a)

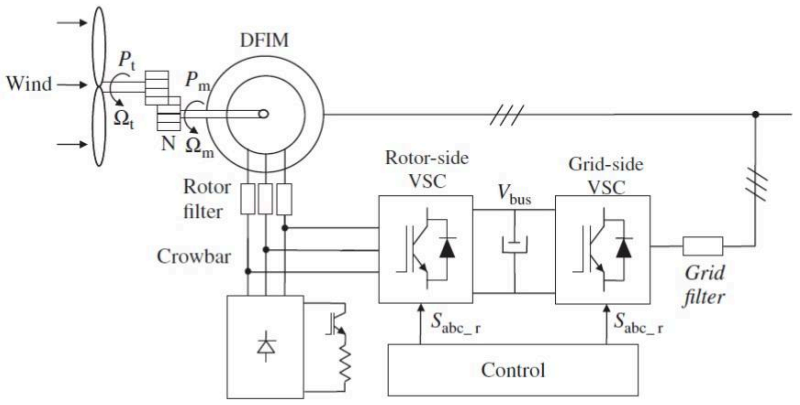

(b)

Figure 5.3 (a) *System equipped with three-phase DC crowbar protection and* ***(b)*** *one phase equivalent circuit of the system when the crowbar is activated*

Is then diverted to the crowbar and the rotor converter is switched off. Figure 5.7b shows the equivalent circuit of the system. As can be seen, when the crowbar is activated, the circuit becomes an impedance divider. In Figure 10.47a, the crowbar comprises a rectifier, a controlled switch and a resistance. There are several alternative crowbar topologies to the crowbar shown in this figure.

The sequence of events that typically occurs during severe voltage dips can be summarised as follows:

1. The DFIM is generating power at steady state at one specific operating point.

2. When the voltage dip occurs, there are a few milliseconds (typically 0.5–5) until the wind turbine's control detects the dip. Thus, during this period the system cannot guarantee control and, in general,there is a high rise of currents through the rotor converter, which also provokes a DC bus voltage increase. The dip is detected by supervising the following anomalies:

(a) overcurrent in the rotor,

(b) overvoltage in the DC link,

(c) grid voltage drop, detected by PLLs or synchronising methods.

3. Once the dip has been detected, the crowbar is activated quickly, which demagnetizes the machine.The rotor converter is inhibited, keeping it safe and ensuring that the entire rotor current circulates through the crowbar. Depending on the machine's design, the time during which the crowbar is active can range for several cycles.

4. Once the flux has decayed and the available converter voltage can control the machine, the crowbar is disconnected and the rotor converter is activated again. In general, because at this moment the flux has not been totally damped, it is preferable to contribute to the total stabilisation of the stator flux by injecting demagnetizing rotor currents by control. At the same time, as demanded by the grid codes, it is possible to provide progressively reactive power through the stator by increasing the corresponding d rotor current component. This situation will last until the grid voltage is progressively recovered, the fault is cleared, and normal operation is resumed.

The resistance of the crowbar $\mathbf{R_{crow}}$ must be chosen carefully. In general, it can be selected by a simulation-based analysis that attempts to find a compromise between the following aspects:

- If a very low value is chosen, the current during the dip will be very large. Thus, the crowbar elements should be oversized and the electromagnetic torque will present a big peak.
- If the resistance is too big, the crowbar will not pull the rotor voltage low enough and the rotor current will circulate across the rotor converter via its freewheeling diodes, even if it is inactive, increasing the DC bus voltage.

Therefore,it is very important that the resistance is sufficiently high that the diodes of the rotor converter do not operate, thus allowing the entire rotor current to circulate through the crowbar resistance.

CHAPTER 6

MODELLING

6.1 INTRODUCTION: As the stator winding of DFIG is connected directly to the infinite grid, the magnitude and frequency of stator voltage can be approximately considered to be constant.Thus we shall adopt vector control method applied to the rotor side converter.

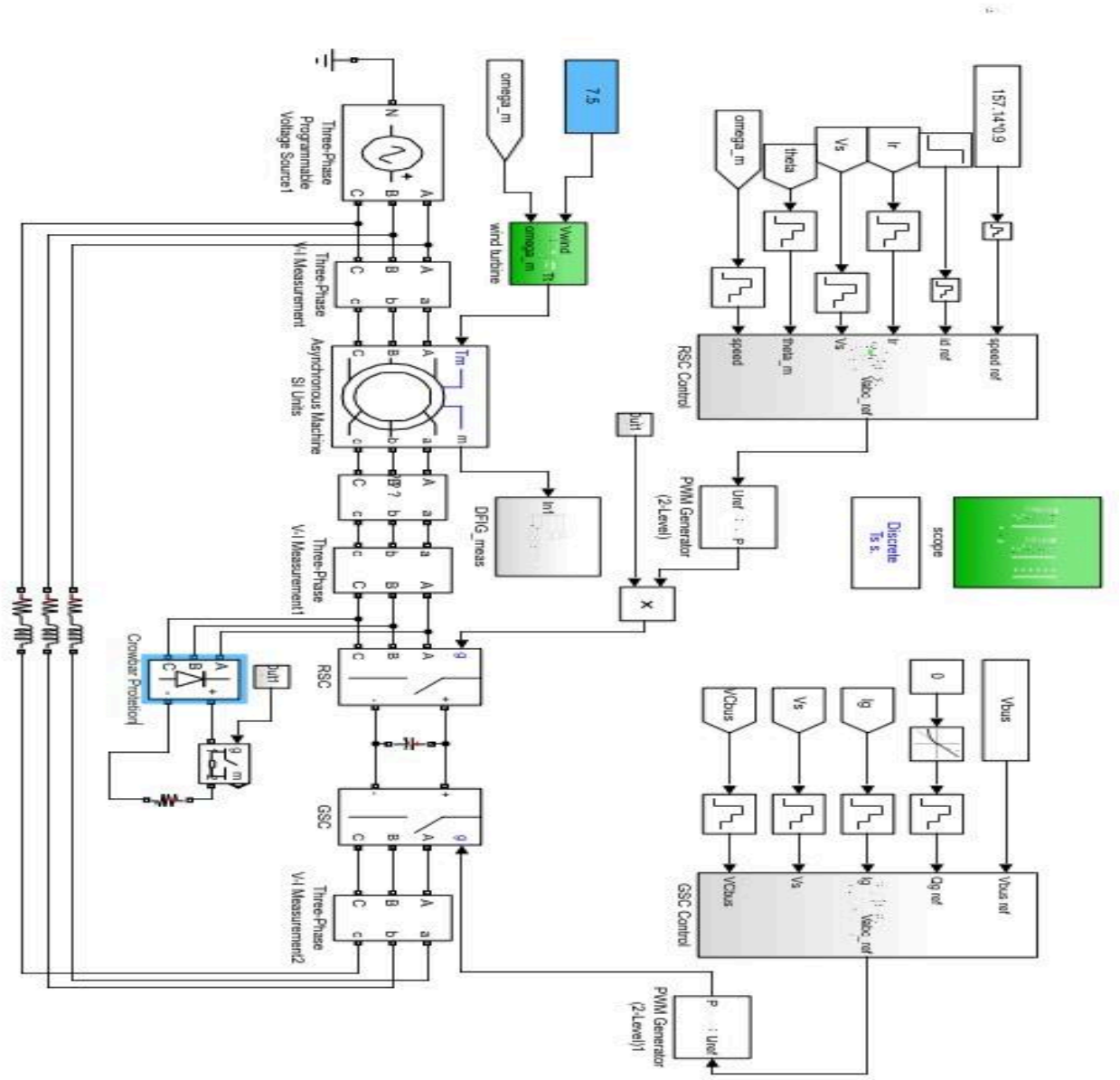

FIGURE 6.1 *Vector control of a DFIG with crowbar protection*

6.2 MATHEMATICAL MODELLING OF WIND TURBINE: The aerodynamic model represents the power extraction of the rotor, calculating the mechanical torque as a function of the airflow on the blades. The wind speed can be considered as the averaged incident wind speed on the swept area by the blades with the aim of evaluating the average torque in the low speed axle.

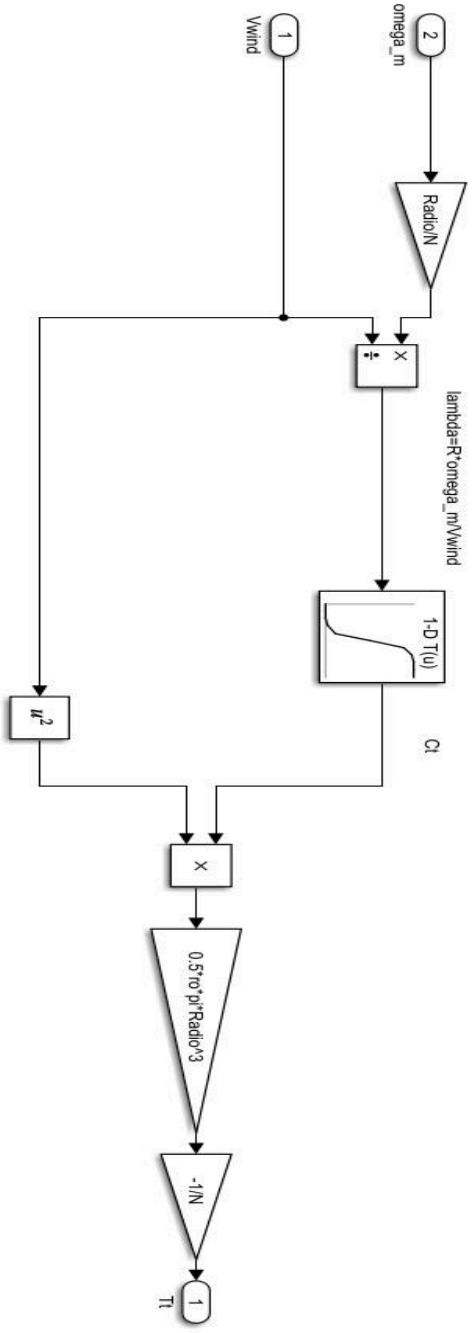

FIGURE 6.2 *Wind turbine model*

Depending on the output torque of the turbine an indirect speed control mechanism has also been adopted for maximum power point tracking,which has been included as a part of the rotor side converter control.

6.3 GRID SIDE CONVERTER MODEL: It contains the d-axis loop,used for dc-link voltage control and the q-axis loop,used for reactive power or grid voltage support control.

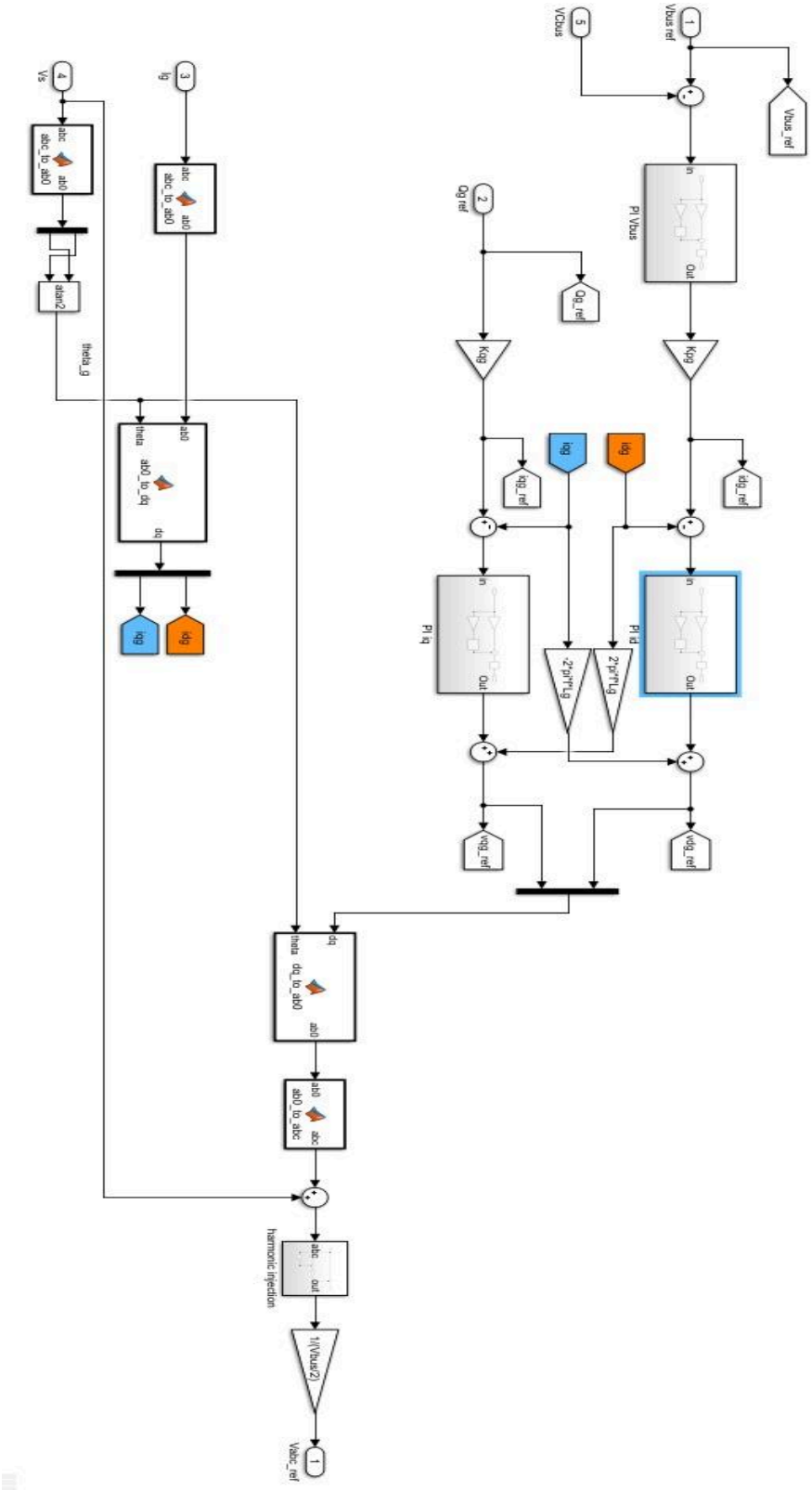

FIGURE 6.3 *GSC control scheme*

P-I controller is the most primitive and highly used controller in power applications for its simplicity and easy applicability. The P-I controllers used in this model have been designed using matlab toolbox as follows,

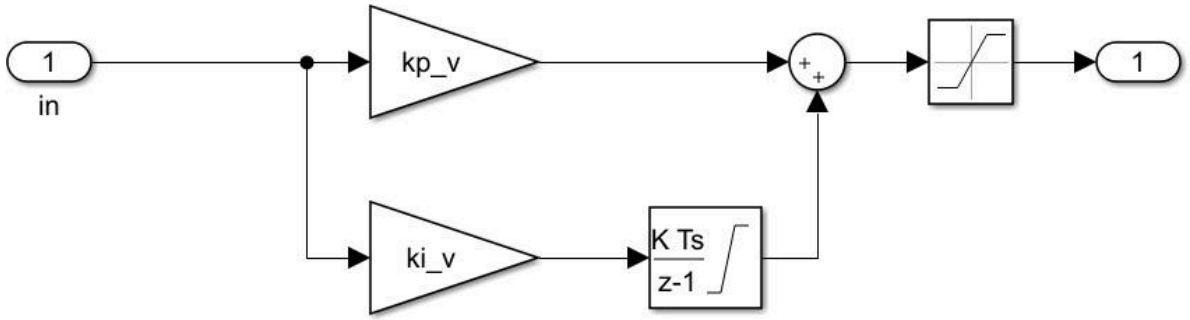

FIGURE 6.4 *P-I controller mathematical model*

The conventional vector control method for the GSC has a nested-loop structure consisting of a faster inner current loop and a slower outer loop.The d -axis voltage is only effective for reactive power or i_q control, and the q -axis voltage is only effective for active power or i_d control. Thus, the conventional control method relies mainly on the compensation terms rather than the PI loops to regulate the d- and q-axis currents via a competing control strategy.

6.4 ASYNCHRONOUS MACHINE MODEL: Here we find that the stator of the DFIG is fed from a Source through a step-down transformer. The source readings are as follows: Phase-to-phase voltage (V_{ph_rms})= 400V, 50Hz. The line resistance in the stator side is 5MΩ and has been put through a block. We find V_{abc_stator} directly from this model and putting V_{abc_stator} and I_{abc_stator} through the 3 phase instantaneous power measurement block gives us the stator active and reactive power.

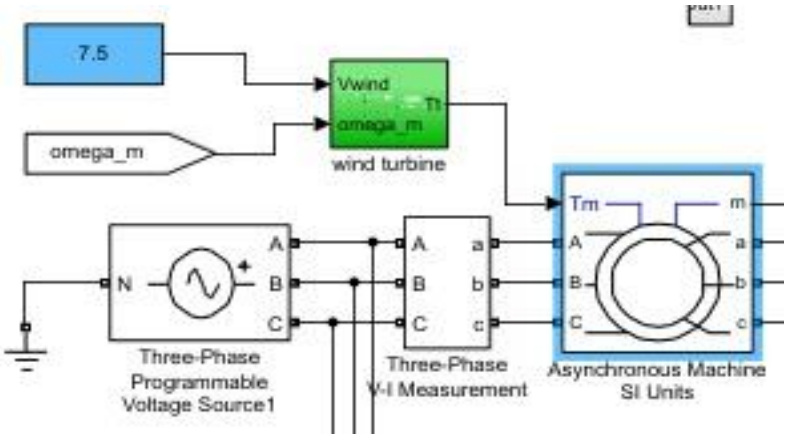

FIGURE 6.5 *Asynchronous machine with 3 phase source*

The DFIG shown in fig 6. Is a 50 Hz machine and maximum rated speed is 1500 rpm. We provide default speed of 1500 rpm to the generator and multiply it with (2*pi)/60 to make it rad/s.

6.5 ROTOR SIDE CONVERTER CONTROL: It contains a d-axis inner loop for controlling d-axis rotor currents and q-axis outer loop for speed control. Along with the conventional P-I controller an indirect speed control method has also been adopted for maximum power point tracking.

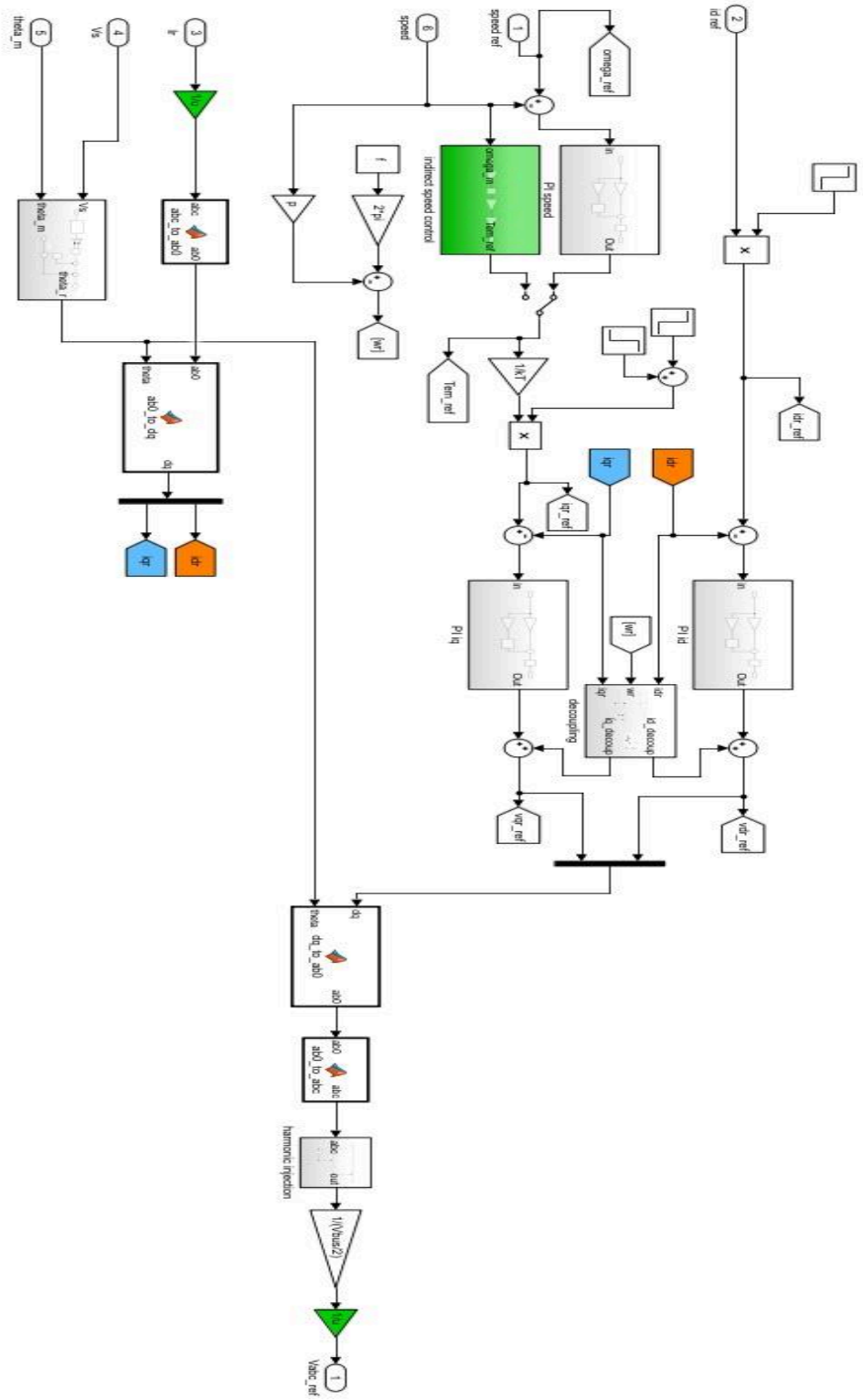

FIGURE 6.6 *Rotor side converter control scheme*

It can easily be shown that theWTis dynamically stable around any point of the maximum power curve of Zone 2.Considering this stability property, the aerodynamic torque T_t can be kept in the maximum power curve in response to wind variations, if the electromagnetic torque T_{em} is controlled in a way to follow this curve.

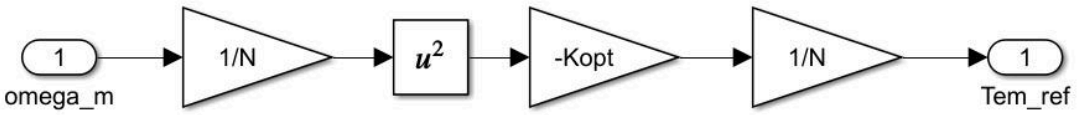

FIGURE 6.7 *Indirect speed control*

$$T_t = K_{opt}\Omega_t^2 \tag{6.1}$$

Where, $K_{opt} = \frac{1}{2}\rho\pi\frac{R^5}{\lambda_{opt}^3}C_{p,max}$

It results in an optimal torque evolving as a quadratic function of the wind turbine speed.

The RSC also comes with a dynamic decoupling circuit that helps in complete decoupling of the d and q components of the rotor current.

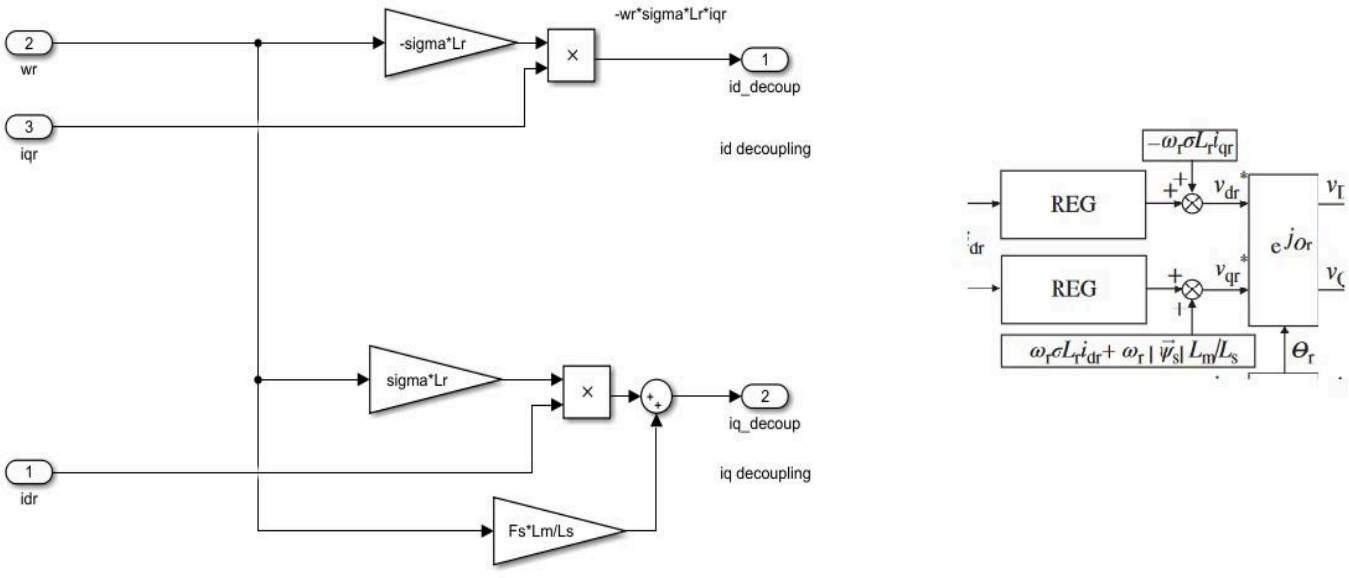

FIGURE 6.8 *Decoupling between d and q component of rotor current*

6.6 SYMMETRICAL VOLTAGE DIP SIMULATION: A symmetrical voltage dip is created using block parameter adjustments of the three phase programmable voltage source in Matlab.The dip is of ten percent of rated voltage and it starts from time t=0 till time t=3 sec.Fundamental harmonics are also included which are assumed to be ten times bigger. The recovery voltage is assumed to be a ramp of recovery rate of 15 Pu/s and it starts from time t=3.5 sec till time t=4.17 sec.

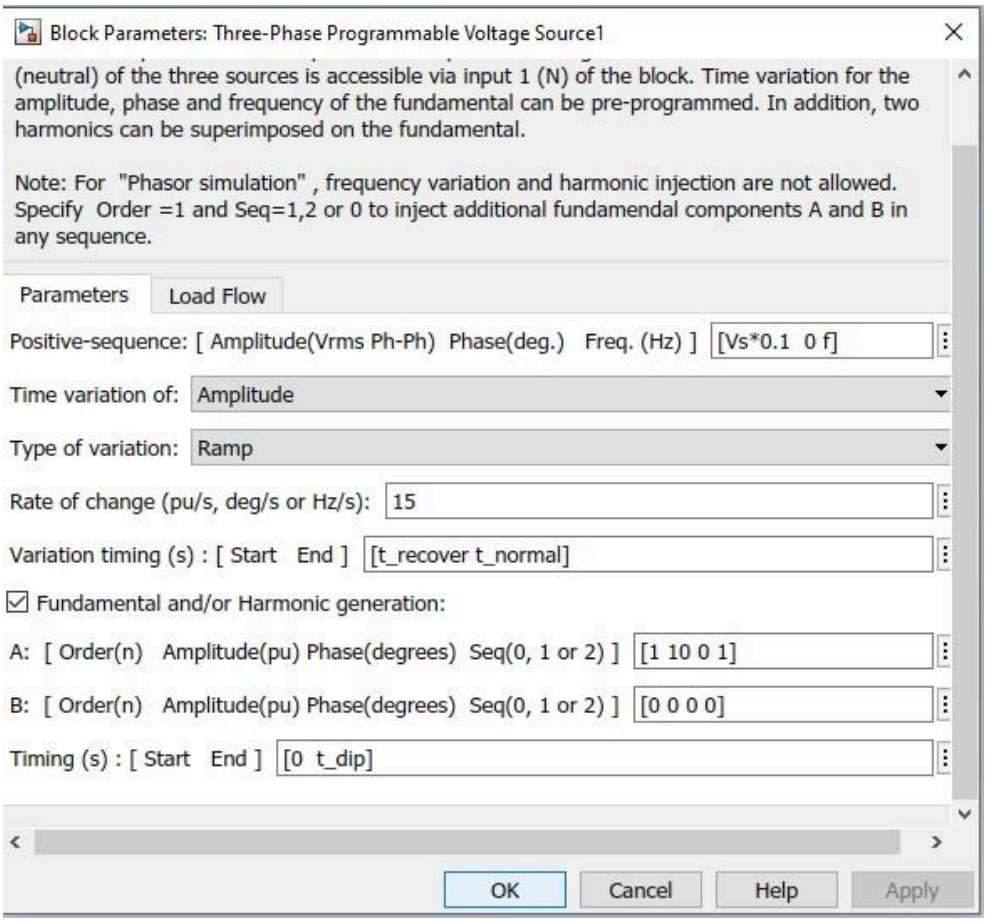

FIGURE 6.10 *Block parameters for three phase programmable voltage source*

6.7 SIMULATION OF CROWBAR PROTECTION: The crowbar protection assembly is made up of diode, resistor and a triggering switch. As per the limited scope and time for the sake of completion of the thesis the detection of the voltage dip has been made manually depending on the specifications of the dip. This is connected in parallel with RSC. The basic operating principle is whenever the

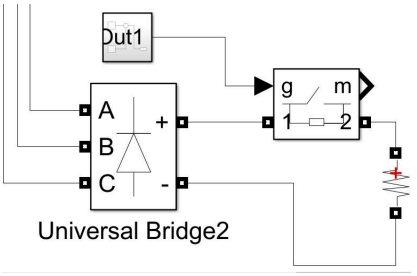

FIGURE 6.11 *Crowbar protection assembly*

voltage dip comes, the RSC should be disconnected and the Crowbar should become active. So that the high currents do not pass through the RSC resulting in complete loss of control. Similarly when the dip has passed the crowbar should get deactivated and the RSC should be connected as it was previously.

a) b)

FIGURE 6.12 *a) Crowbar enable b) RSC enable*

6.8 INITIALIZATION PROGRAM: The program contains all the static and dynamically calculated values of all the model parameters. For the proper operation of the model it needs to run first even before the simulation.

```
% DFIG parameters -> Rotor parameters referred to the stator side
f = 50;            % Stator frequency (Hz)
Ps = 2e6;          % Rated stator power (W)
n = 1500;          % Rated rotational speed (rev/min)
Vs = 690;          % Rated stator voltage (V)
Is = 1760;         % Rated stator current (A)
Tem = 12732; % Rated torque (N.m)
p=2;               % Pole pair
u = 1/3;           % Stator/rotor turns ratio
Vr = 2070;       % Rated rotor voltage (non-reached) (V)
smax = 1/3;     % Maximum slip
Vr_stator = (Vr*smax) *u;     % Rated rotor voltage referred to stator (V)
Rs = 2.6e-3;     % Stator resistance(ohm)
Lsi = 0.087e-3; %  Leakage inductance (stator & rotor) (H)
Lm = 2.5e-3; %  Magnetising inductance (H)
Rr = 2.9e-3; % Rotor resistance referred to stator (ohm)
Ls = Lm + Lsi; % Stator inductance (H)
Lr = Lm + Lsi; % Rotor inductance (H)
% Vbus = Vr_stator*sqrt(2); % DC de bus voltage referred to stator (V)
Vbus = 1150; % as in tutorial 4

sigma = 1-Lm^2/(Ls*Lr);
```

```
Fs = Vs*sqrt(2/3)/(2*pi*f);  % Stator Flux (approx.) (Wb)
J = 127; % Inertia, originally 127, reduced by 2 to make the response faster
D = 1e-3; %damping

fsw = 4e3;
Ts =  1/fsw/50;
kT = -1.5*p*(Lm/Ls)*Fs; % kT, coef of output of the speed controller

tau_i = (sigma*Lr)/Rr;
tau_n = 0.05;
wni = 100*(1/tau_i);
wnn = 1/tau_n;

kp_id = (2*wni*sigma*Lr)-Rr;
kp_iq = kp_id;

ki_id = (wni^2)*Lr*sigma;
ki_iq = ki_id;

kp_n = (2*wnn*J)/p; %kp_n = (2*wnn*J)/p;
ki_n = (wnn^2)*J/p; %ki_n = (wnn^2)*J/p;


% Three blade wind turbine mode
N = 100; % Gearbox ratio
Radio= 42; % blade radius
ro= 1.225; % Air density

% Cp and Ct curves
beta=0;  % Pitch angle
ind2=1;
for lambda=0.1:0.01:11.8
   lambdai(ind2)= (1./((1./(lambda-0.02.*beta) + (0.003./ (beta^3+1)))));
                        Cp(ind2)=0.73*(151./lambdai(ind2)      -      0.58*beta      -
0.002.*beta^2.14-13.2).*(exp(-18.4./lambdai (ind2)));
   Ct(ind2)=Cp(ind2)/lambda;
   ind2=ind2+1;
end
tab_lambda=[0.1:0.01:11.8];
% Kopt for MPPT
Cp_max = 0.44;
lambda_opt = 7.2;
Kopt = ((0.5*ro*pi* (Radio^5) *Cp_max)/(lambda_opt^3));
% Power curve in fucntion of wind speed
```

```
P = 1.0e+06 *[0,0,0,0,0,0,0,0.0472,0.1097,0.1815,0.2568,0.3418, ...
          0.4437,0.5642, 0.7046, 0.8667,1.0518,1.2616, 1.4976, 1.7613,2.0534,...
          2.3513,2.4024,2.4024,2.4024, 2.4024,2.4024,2.4024];
V = [0.0000,0.5556,1.1111,1.6667,2.2222,2.7778,3.3333,3.8889, 4.4444,...
   5.0000,5.5556,6.1111,6.6667,7.2222,7.7778,8.3333,8.8889,9.4444, ...
   10.0000,10.5556,11.1111, 11.6667,12.2222,12.7778,13.3333, 13.8889,...
   14.4444,15.0000];
 figure
 subplot(1,2,1)
 plot(tab_lambda, Ct, 'linewidth',1.5)
 xlabel('\lambda', 'fontsize',14)
 ylabel('Ct', 'fontsize',14)
 subplot(1,2,2)
 plot (V, P, 'linewidth', 1.5)
 grid
 xlabel('Wind speed (m/s)', 'fontsize',14)
 ylabel('Power (W)', 'fontsize',14)


% Grid side converter
Cbus = 80e-3; % DC bus capacitance
Rg = 20e-6; % Grid side filter's resisatance
Lg = 400e-6; % Grid side filter's inductance
Kpg = 1/(1.5*Vs*sqrt(2/3));
Kqg = -Kpg;

% PI regulators
tau_ig = Lg/Rg;
wnig = 60*2*pi;

kp_idg = (2*wnig*Lg)-Rg;
kp_iqg = kp_idg;
ki_idg = (wnig^2)*Lg;
ki_iqg = ki_idg;

kp_v = -1000;
ki_v = -300000; %ki_v = -300000;

Rcrowbar = 0.2; % crowbar circuit resistance
Tcrowbar = 0.1; % crowbar duration 0.1s

t_dip= 3;
t_recover = 3.5;
t_normal = 4.17;
```

CHAPTER 7

SIMULATION RESULTS AND CONCLUSIONS

7.1 POWER- SPEED CHARACTERISTICS OF THE WIND TURBINE:

The 2.5 MW wind turbine so designed has been matched with the commercially available NORDEX N80 2.5 MW VSWT.

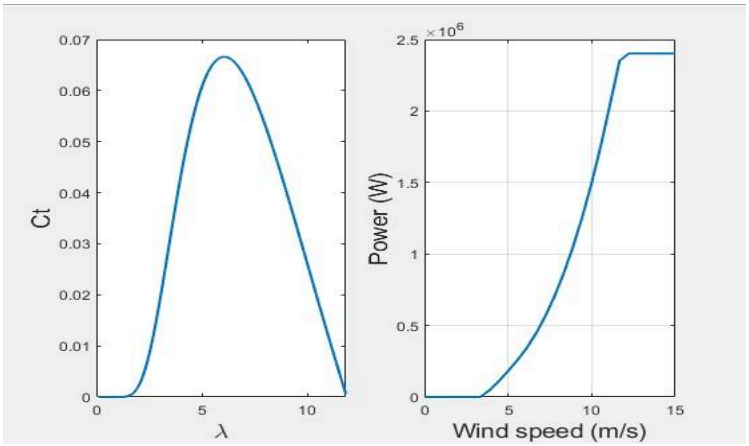

FIGURE 7.1 *Characteristics of 2.5 MW VSWT*

7.2 VOLTAGE DIP ANALYSIS:

7.2.1 With indirect speed control:

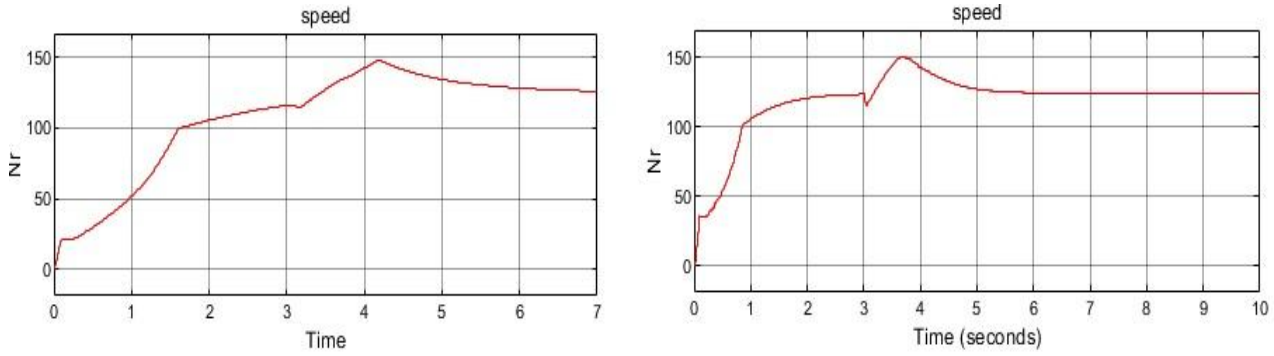

FIGURE 7.2 a) Speed time characteristics With Crowbar

b) Speed time characteristics without crowbar

In figure 7.2 it is evident that without active crowbar maximum speed is obtained faster however in this indirect mode of speed control with active crowbar the speed variations are smoother and gradual.

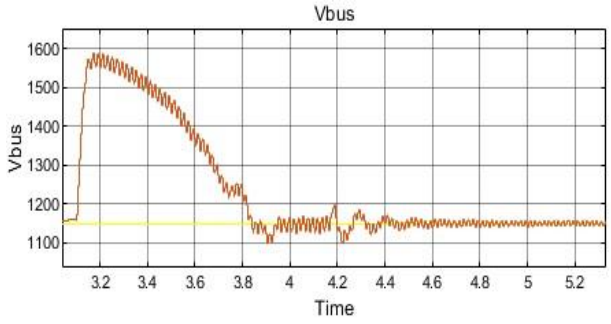

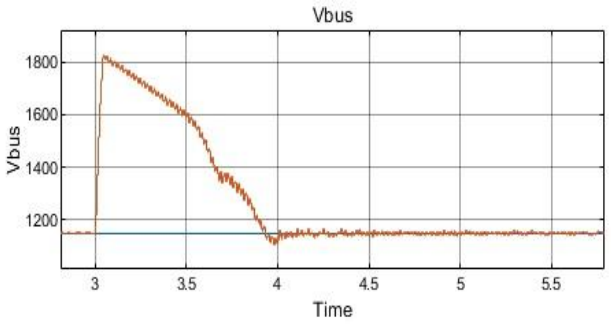

FIGURE 7.3 a) DC link voltage with Active crowbar

b) Dc link voltage without Active crowbar

It is evident from the figure 7.3 that under indirect speed control scheme with active crowbar the overshoot in dc bus voltage during the voltage dip is minimized.

0

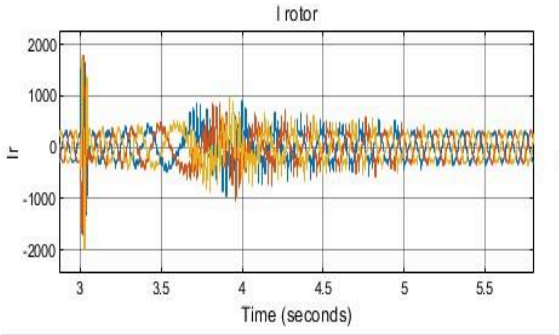

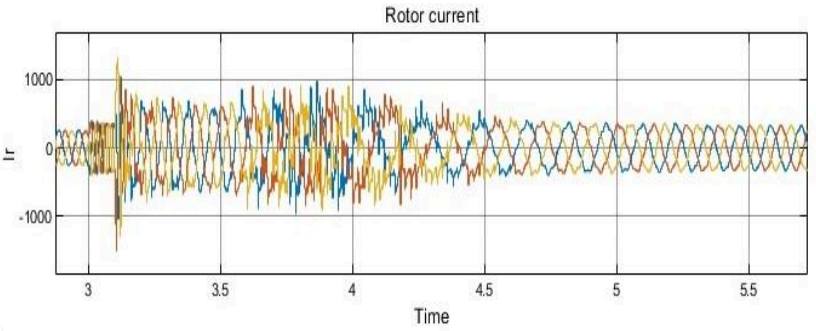

FIGURE 7.4 a) Rotor current without Active crowbar

b) Rotor current with Active crowbar

Rotor currents are seen to be less distorted during LVRT and recovery phase, with an active crowbar protection under indirect speed control scheme,in figure 7.4.

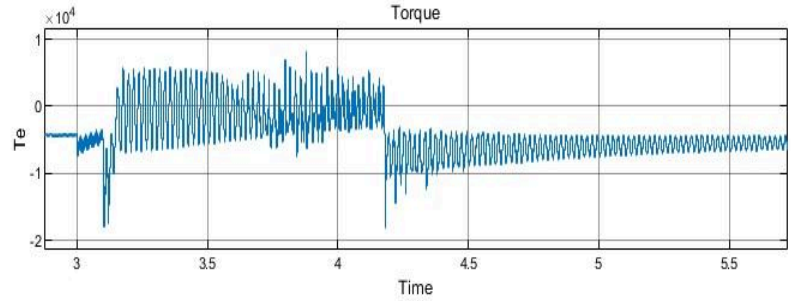

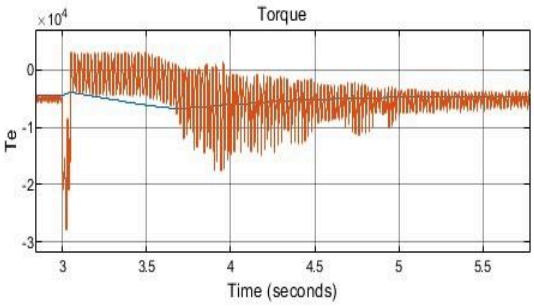

FIGURE 7.5 a) Torque characteristics with active Crowbar

b) Torque Characteristics Without crowbar

It is evident from figure 7.5 that due to the active crowbar protection some amount of active power and hence torque is lost. Also Load tracking is little degraded due to active crowbar protection in the indirect speed control scheme.

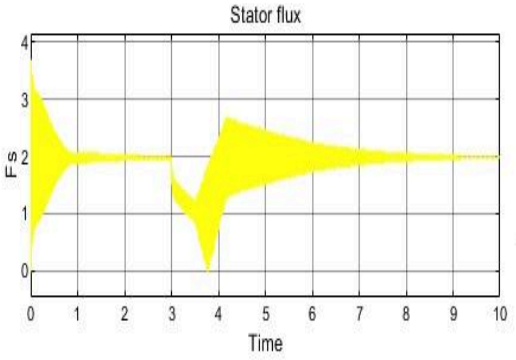

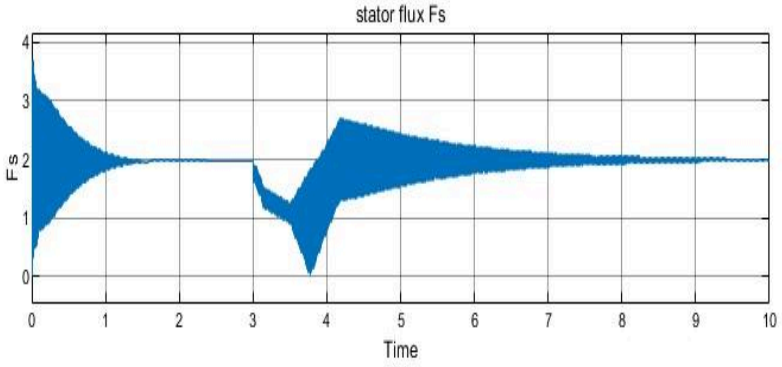

FIGURE 7.6 a) Stator flux without Crowbar protection

b) Stator flux with active crowbar protection

Flux pattern remains almost similar in both case as seen in figure 7.6.

7.2.2 with PI speed controller:

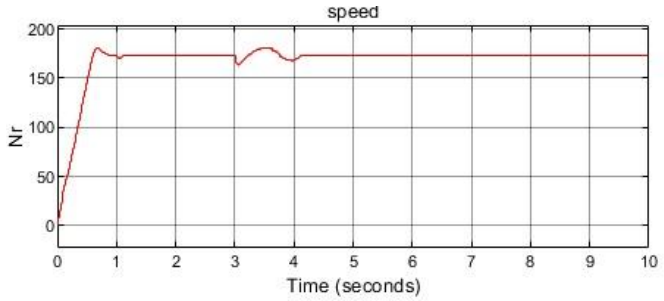

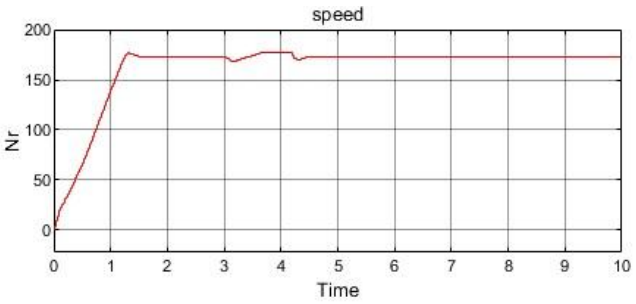

FIGURE 7.7 a) Speed characteristics without Active crowbar protection

b)Speed characteristics with active crowbar protection

With crow bar protection Speed tracking is smoother and with gradual speed variation. Under PI controller speed regulation scheme hypersynchronous generation is observed.

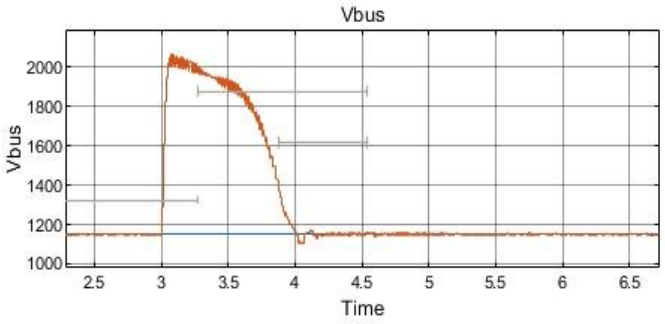

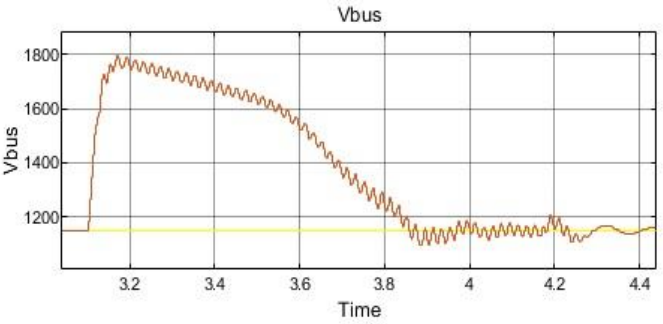

FIGURE 7.8 a) DC link voltage without active Crowbar protection

b) DC link voltage with Active crowbar protection

Voltage overshoot in dc link during LVRT and recovery is minimised using crowbar as seen in figure 7.8.

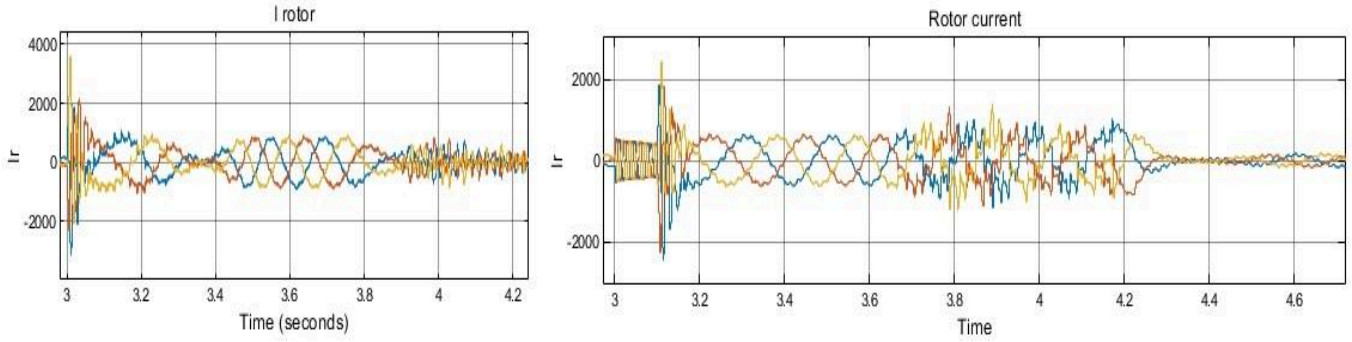

FIGURE 7.9 a) Rotor currents without Crowbar protection

b) Rotor current with active crowbar protection

Rotor currents are seen to be less distorted during LVRT and recovery phase, with an active crowbar protection under indirect speed control scheme,in figure 7.9.

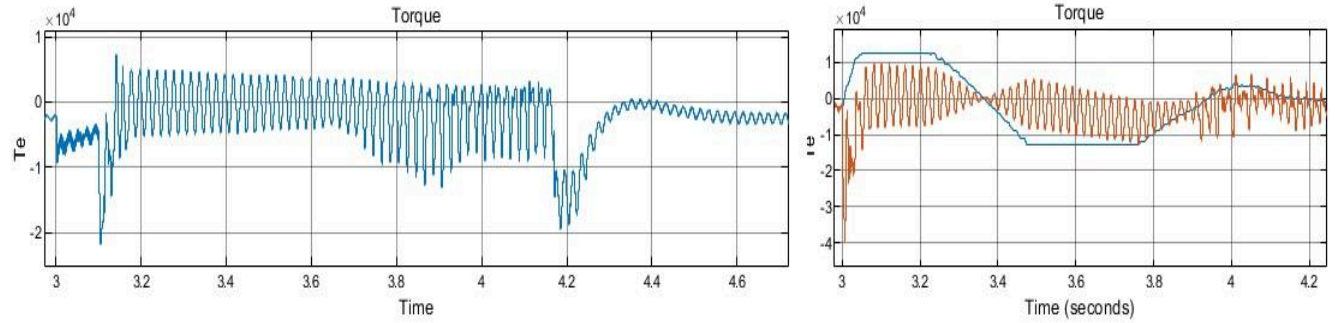

FIGURE 7.10 a) Torque characteristics with Active Crowbar protection

b)Torque characteristics without active crowbar protection

Some amount of torque is lost due to crowbar protection.Load tracking is better without crowbar protection as seen in figure 7.10.

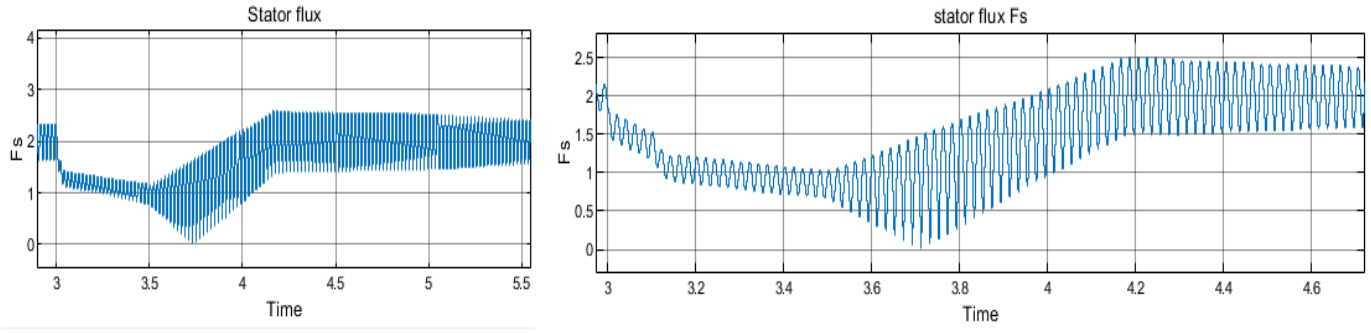

FIGURE 7.11 a) Flux characteristics Without Crowbar

b) Flux characteristics with active crowbar protection

Flux pattern remains almost similar in both cases as seen in figure 7.11.

7.2.3 Comparison between crowbar currents:

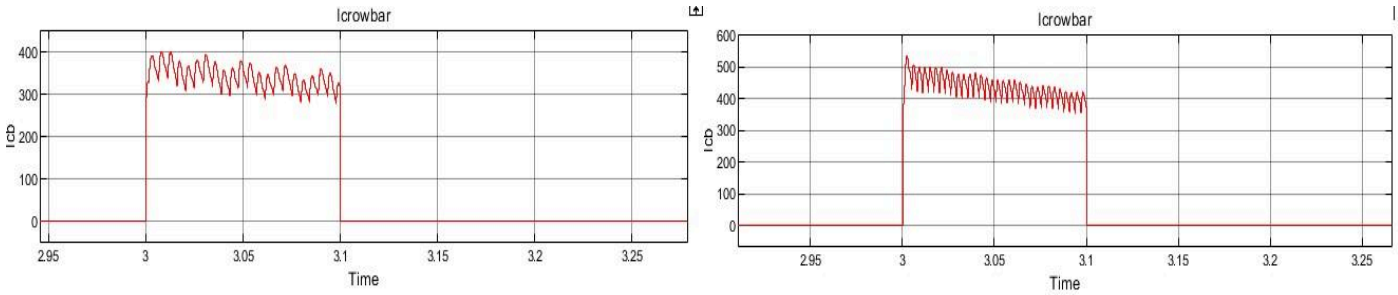

FIGURE 7.12 a) crowbar current with Indirect Speed controller b) Crowbar current with PI controller

The two major aspects of crowbar protection is the value of crowbar resistance and the crowbar activation time. In the above example the crowbar resistance value is set to be 5 Ω and the crowbar is active for 0.1 seconds. It is evident from figure 7.12 that with an indirect speed controller the crowbar current is less as compared to that of a PI-controller.

7.3 CONCLUSIONS: This article presents the dynamic analysis of a DFIG-based wind farm connected to a test system. Based on the results, when the wind turbines must keep connected during faults, the crowbar resistance value should be high enough to guarantee lower reactive power consumption. However, when the fault occurs close to the wind farm, the influence of the crowbar resistance is lower. Other observations during the LVRT with a hypersynchronous speed, are listed below,

i) With the active crowbar protection flux and voltage recovery is accelerated as compared to the model without any active crowbar in case of a symmetrical voltage dip.

ii) The distortion in stator flux, developed torque and dc link voltage is reduced to a greater extent during LVRT as well as during recovery.

iii)Rotor currents are reduced and are much more symmetrical even during LVRT and recovery with an active crowbar.

iv)With indirect speed controllers the optimum speed tracking is gradually attained whereas with PI speed controllers the machine reaches reference speed abruptly resulting in sharp spikes in dc link voltage. However both the methods proved to be a good avenue for optimum speed tracking mechanism.

v) With an indirect speed controller the crowbar current during LVRT is reduced, so we can use a crowbar resistance of smaller ratings with an indirect speed controller.

7.4 FUTURE AVENUES FOR RESEARCH:

i) Ideally the crowbar resistance should be calculated dynamically with two restraining conditions ie. whenever rotor currents go beyond limit or whenever the dc link voltage goes beyond the limits the crowbar should get activated. So depending on the reactive power demand the crowbar resistance value should be estimated. However in this thesis I have used a constant crowbar resistance value for the sake of simplicity and to meet the time boundation for completion of this thesis.

ii) A braking chopper is an electric device connected to the DC-link bus of the back-to-back converters to prevent an uncontrolled increase of their voltage

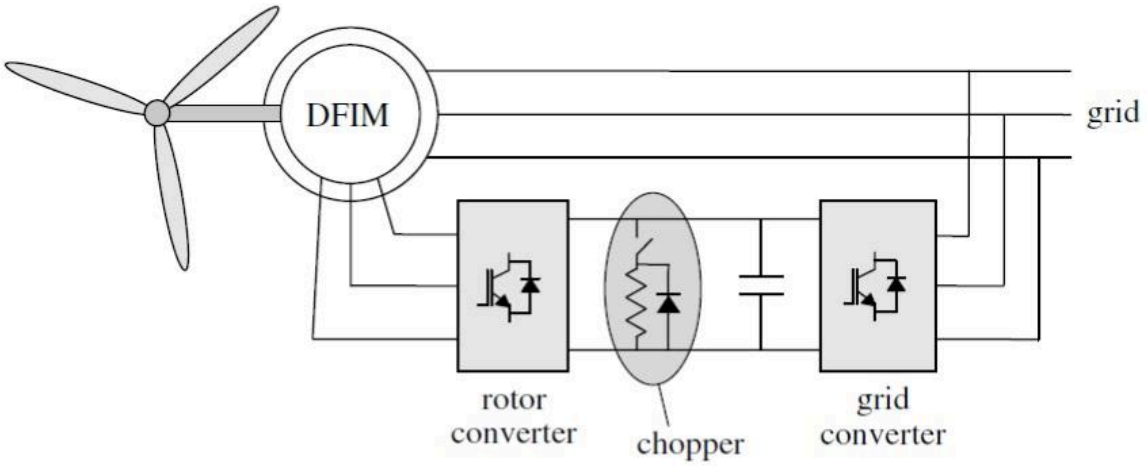

FIGURE 7.13: System equipped with braking chopper

The braking chopper is made up of a resistor that can be connected or disconnected by means of a switch. A freewheeling diode is also necessary to prevent overvoltages in the switch when it is turned off. Control of the switch is often made by an ON–OFF (also known as hysteresis) controller: when the actual DC bus voltage exceeds a specified level, the resistor is connected and the surplus energy is dissipated. The resistor is kept connected until the voltage drops below a minimum specified level, when the resistor is disconnected.The installation of a braking chopper in modern commercial turbines to protect the converters from overvoltages in the DC link is more and more common. It can be installed alone or in combination with an active crowbar.

7.5 REFERENCES:

[01] Gonzalo Abad, Jesús López, Miguel Rodríguez, Luis Marroyo, Grzegorz Iwanski - “Doubly Fed Induction Machine_ Modeling and Control for Wind Energy Generation Applications,” (IEEE Press Series on Power Eng).

[02] Abu-Rub, Haitham Malinowski, Mariusz Al-Haddad, Kamal - “Power Electronics for Renewable Energy Systems, Transportation and Industrial Applications,” Abu-Rub Power Electronics for Renew (2014, John Wiley & Son).

[03] J. Lo´pez, L. Marroyo, E. Gubia, E. Olea, and I. Ruiz, “Ride-through of Wind Turbines with Doubly-Fed Induction Generator Under Symmetrical Voltage Dips,” IEEE Trans. Ind.Electron., Vol. 56, pp. 4246–4254, October 2009.

[04] R. Pena,J.C.Clare,G. M. Asher-”Doubly fed induction generator using back-to-back PWM converters and its application to variable speed wind-energy generation,”IEE Proc.-Electr. Power Appl., Vol. 143, No 3, May 1996.

[05] J. B. Ekanayake, L. Holdsworth, X. G.Wu, and N. Jenkins, “Dynamic Modeling of Doubly Fed Induction Generator Wind Turbines,” IEEE Trans. Power Systems, Vol. 18, No. 2, pp. 803–809, May 2003.

[06]Shuhui Li, Senior Member, IEEE, Timothy A. Haskew, Senior Member, IEEE, Keith A. Williams, and Richard P. Swatloski-”Control of DFIG Wind Turbine With Direct-Current Vector Control Configuration,”IEEE Trans. On Sustainable Energy, Vol. 3, No. 1, January 2012.

[07] A.V.Timbus, P.Rodriguez, R.Teodorescu, M.Liserre,andF.Blaabjerg, “Control strategies for distributed power generation systems operating on faulty grid,” in Proc. IEEE Int Industrial Electronics Symp, vol. 2, 2006, pp. 1601–1607.

[08] L. Xu and Y. Wang, “Dynamic modelling and control of DFIG-based wind turbines under unbalanced network conditions,” IEEE Trans. Power Syst., vol. 22, No. 1, pp. 314–323, Feb. 2007.

[09] Badrul H. Chowdhury and Srinivas Chellapilla, “Double-fed induction generator control for variable speed wind power generation,” Electric Power Systems Research, vol. 76, no. 9-10, pp. 786-800, June 2006.

[10] H.Akagi, Y.Kanazawa,and A.Nabae, “Instantaneous reactive power compensators comprising switching devices without energy storage components,” IEEE Trans. Ind. Appl.,vol. 20, no. 3, pp. 625–630, 1984.

[11] M. Yamamoto and O. Motoyoshi, “Active and reactive power control for doubly fed wound rotor induction generator,” IEEE Trans. Power Electronics, vol. 6, no. 4, pp. 624-629, Oct 1991.

[12] A.Tapia, G. Tapia, J.X. Ostolaza and J.R. Saenz, “Modelling and control of a wind turbine driven doubly fed induction generator,” IEEE Trans. Energy Conversion, vol. 18, no. 2. pp. 194 – 204, June 2003.

[13] Jamal A. Baroudi, Venkata Dinavahi, and Andrew M. Knight, “A review of power converter topologies for wind generators,” Int. Journal of Renewable Energy, vol.32, no.14, pp.2369–2385, 2007.

[14] Zhe Chen, Josep M. Guerrero, and Frede Blaabjerg. “A Review of the State of the Art of Power Electronics for Wind Turbines” in IEEE Transactions on Power Electronics, VOL. 24, NO. 8, AUGUST 2009, DOI:10.1109/TPEL.2009.2017082.

[15] Sergei P, Andrea T, and Alerto T, “Power control of a doubly fed induction machine via output feedback,” Control Engineering Practice, vol. 12, pp. 41-57, Jan. 2004.
[16] Some references and figures necessary for theory explanation taken from the website of “https://www.researchgate.net/”.

[17] https://www.investindia.gov.in/sector/renewable-energy

[18] https://www.explainthatstuff.com/windturbines.html